

## Synthesis, Structure, and Ligand Exchange Reactions of Tetramethyleneethane Complexes of Cobalt

Paulina Aguirre-Etcheverry, Andrew E. Ashley, Gábor Balázs, Jennifer C. Green, Andrew R. Cowley, Amber L. Thompson, and Dermot O'Hare\*

Chemistry Research Laboratory, Department of Chemistry, University of Oxford, Mansfield Road, Oxford, OX1 3TA, U.K.

Received June 24, 2010

The synthesis of  $(\eta^3:\eta^3\text{-TME})[\text{Co}(\text{CO})_3]_2$  (**1**) was achieved using 2,3-bis(bromomethyl)-1,3-butadiene ( $\text{TMEBr}_2$ ) as the tetramethyleneethane (TME) ligand precursor and  $\text{Na}[\text{Co}(\text{CO})_4]$ . Solution NMR studies suggested an  $\eta^3:\eta^3$ -configuration, which has been confirmed in the solid state by single-crystal X-ray diffraction studies. The series of complexes  $(\eta^3:\eta^3\text{-TME})[\text{Co}(\text{CO})_2\text{PR}_3]_2$  ( $\text{R} = \text{Me}$ , **2**;  $\text{R} = \text{Et}$ , **3**;  $\text{R} = n\text{-Bu}$ , **4**;  $\text{R} = \text{Ph}$ , **5**;  $\text{R} = \text{OPh}$ , **6**) were also synthesized by ligand exchange reactions, demonstrating that only one carbonyl may be exchanged for a phosphine group on each metal center. The  $\eta^3:\eta^3$ -configuration of the tetramethyleneethane ligand in these complexes was determined by crystallographic studies. The effect of the electron-donating properties of  $\text{PR}_3$  was studied by cyclic voltammetry (CV) and infrared spectroscopy. The greatest degree of electron donation was seen when  $\text{R} = \text{Et}$  (**3**) and lowest when  $\text{R} = \text{Ph}$  (**5**) or  $\text{R} = \text{OPh}$  (**6**). Electronic communication between the metal centers was observed by CV. The chemical oxidation of **1** resulted in a highly unstable species that decomposed to  $\{[(\text{CO})_2\text{Co}]\text{TME}[\text{Co}(\text{CO})_3]\}^+[\text{BF}_4]^-$  (**1<sup>+</sup>d**), determined by its crystal structure. The synthesis of  $(\eta^4:\eta^4\text{-TME})[\text{CoCp}^*]_2$  (**7**) has been achieved using a dipotassium 2,3-bis(methylene)-1,3-butanediyl ( $\text{TMEK}_2$ ) synthon. NMR studies suggested that **7** adopts an unusual  $\eta^4:\eta^4$ -configuration, which was confirmed with the aid of crystallographic studies. DFT calculations were performed in order to rationalize the bonding for **1**, **7**, and hypothetical  $(\eta^4:\eta^4\text{-TME})[\text{CoCp}]_2$  (**8**). The large energy difference between the two coordination isomers **1** and **1a** confirmed the  $\eta^3:\eta^3$ -configuration. For isomers **7/7a** and **8/8a**, the energy difference between the two isomers (ca.  $15 \text{ kJ mol}^{-1}$ ) is in favor of the  $\eta^4:\eta^4$ -configuration. For complexes **1<sup>+</sup>** and **8<sup>+</sup>**, the calculations suggested complete delocalization on the system when one electron was removed.

### Introduction

Allyl-containing transition metal complexes represent some of the earliest examples of organometallic complexes.<sup>1</sup> These types of compounds have become of increased interest because of their importance in preparative organic chemistry and catalytic reactions; the high catalytic activity is in part due to the coordination flexibility of allyl–metal bonding.<sup>2</sup>

On a general basis, organometallic compounds containing the allyl ( $\text{C}_3\text{H}_5$ ) moiety can be classified as follows:  $\sigma$ -allyl, where a terminal carbon atom is  $\sigma$ -bonded to the metal atom with a localized double bond between the two remaining carbon atoms, e.g.,  $(\sigma\text{-C}_3\text{H}_5)\text{Mn}(\text{CO})_5$ ;<sup>3</sup>  $\mu$ -allyl, where the allyl group bridges two metal atoms, being  $\sigma$ -bonded to one metal atom through a terminal carbon and to the second metal atom through interaction of the allyl double bond with

the metal orbitals, e.g.,  $(\text{C}_3\text{H}_5)_4\text{Cr}_2$ ;<sup>4</sup> or  $\pi$ -allyl, where the bond between the allyl group and the metal atom is delocalized and multicentric, e.g.,  $(\pi\text{-C}_3\text{H}_5)_2\text{Ni}$ .<sup>5</sup> In some cases, conversion from the  $\sigma$ - to the  $\pi$ -bonded type is possible by heating or UV irradiation.

The  $\text{C}_3\text{H}_5$  ligand has been widely studied, and many monometallic organometallic complexes have been synthesized demonstrating interesting behavior in catalytic reactions, ligand exchange, and polymerization, and as a reagent in organic chemistry.<sup>6</sup> The allyl-metal complexes can be of the pure  $\pi$ -allyl

\* Author for correspondence. E-mail: dermot.ohare@chem.ox.ac.uk. Tel: +44 (0) 1865 272686. Fax: +44 (0) 1865 285131.

(1) Wilke, G.; Bogdanov, B.; Hardt, P.; Heimbach, P.; Keim, W.; Kroner, M.; Oberkirc, W.; Tanaka, K.; Steinruc, E.; Walter, D.; Zimmermann, H. *Angew. Chem., Int. Ed. Engl.* **1966**, *5*, 151.

(2) Clarke, H. L. *J. Organomet. Chem.* **1974**, *80*, 369.

(3) Clarke, H. L.; Fitzpatrick, N. J. *J. Organomet. Chem.* **1972**, *40*, 379.

(4) Aoki, T.; Furusaki, A.; Yujiro Tomiie, Y.; Ono, K.; Tanaka, K. *Bull. Chem. Soc. Jpn.* **1969**, *42*, 545.

(5) Clarke, H. L. *J. Organomet. Chem.* **1974**, *80*, 155.

(6) (a) Betz, P.; Dohring, A.; Emrich, R.; Goddard, R.; Jolly, P. W.; Kruger, C.; Romao, C. C.; Schonfelder, K. U.; Tsay, Y. H. *Polyhedron* **1993**, *12*, 2651. (b) Nieman, J.; Pattiasina, J. W.; Teuben, J. H. *J. Organomet. Chem.* **1984**, *262*, 157. (c) Bogdanovi, B.; Borner, P.; Breil, H.; Hardt, P.; Heimbach, P.; Herrmann, G.; Kaminsky, H. J.; W. Keim, W.; Kröner, M.; Müller, H.; Müller, E. W.; Oberkirch, W.; Schneider, J.; Stedefeder, J.; Tanaka, K.; Weyer, K.; Wilke, G. *Angew. Chem., Int. Ed. Engl.* **1963**, *2*, 105. (d) Kurosawa, H. *J. Organomet. Chem.* **1987**, *334*, 243. (e) Gren, C. K.; Hanusa, T. P.; Brennessel, W. W. *Polyhedron* **2006**, *25*, 286. (f) Ray, B.; Neyroud, T. G.; Kapon, M.; Eichen, Y.; Eisen, M. S. *Organometallics* **2001**, *20*, 3044. (g) Carlson, C. N.; Smith, J. D.; Hanusa, T. P.; Brennessel, W. W.; Young, V. G. *J. Organomet. Chem.* **2003**, *683*, 191.

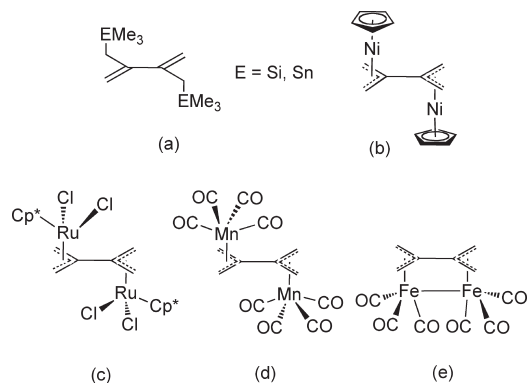


**Figure 1.** (a)  $(\eta^1:\eta^1\text{-TME})[E(\text{CH}_3)_3]_2$  ( $E = \text{Si}^{13}, \text{Sn}^{14}$ ), (b)  $(\eta^3:\eta^3\text{-TME})[\text{NiCp}]_2$ ,<sup>15</sup> (c)  $(\eta^3:\eta^3\text{-TME})[\text{RuCp}^*\text{Cl}_2]_2$ ,<sup>16</sup> (d)  $(\eta^3:\eta^3\text{-TME})[\text{Mn}(\text{CO})_4]_2$ ,<sup>17</sup> (e)  $(\eta^3:\eta^3\text{-TME})[\text{Fe}(\text{CO})_3]_2$ .<sup>18</sup>

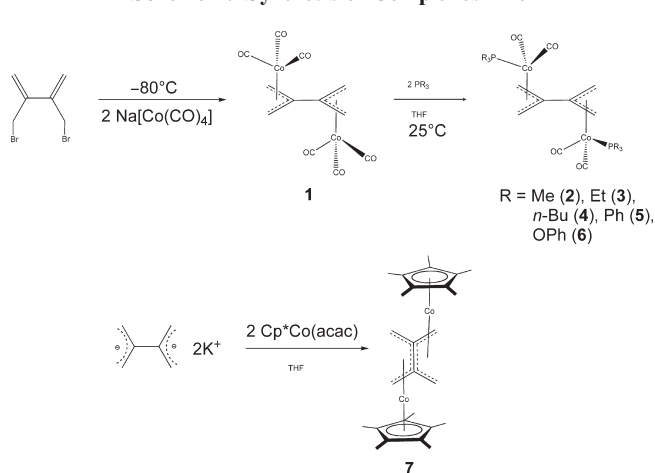
type, such as  $(\pi\text{-C}_3\text{H}_5)_2\text{Ni}$ ,<sup>5</sup>  $(\pi\text{-C}_3\text{H}_5)_3\text{Co}$ ,<sup>7</sup> or  $(\pi\text{-C}_3\text{H}_5)_4\text{Zr}$ .<sup>8</sup> They can also involve other ligands; examples include carbonyls  $(\pi\text{-C}_3\text{H}_5)\text{Co}(\text{CO})_3$ , triphenyl phosphine  $(\pi\text{-C}_3\text{H}_5)\text{Ir}(\text{CO})(\text{PPh}_3)_2$ ,<sup>10</sup> and  $\eta^5\text{-cyclopentadienyl } (\pi\text{-C}_3\text{H}_5)\text{Ni}(\eta^5\text{-Cp})$ .<sup>9b</sup> The allyl fragment can also support substituents ( $\pi\text{-C}_3\text{H}_5$ ), be part of a hydrocarbon ring, or be cyclic.<sup>1,5,6d</sup>

Bimetallic complexes containing two metal centers linked by a bridging ligand may support metal–metal interactions depending on the nature of the ligands. The physical and chemical properties of one of the metal centers can vary significantly due to the vicinity of the other.<sup>11</sup> Applications for these systems may be found in biological processes, molecular electronics, and theoretical studies of electron-transfer processes.<sup>11g,12</sup>

We were interested in studying the metal–metal interactions in bimetallic systems containing bridging allyl moieties. An example of a ligand capable of binding two metal centers is 2,3-dimethyl-1,3-butadiene (TMEH<sub>2</sub>) since the proximity of the two allyl fragments should facilitate the communication of the metal centers; the few known organometallic complexes with a TME fragment bonded in an  $\eta^1:\eta^1$ - and  $\eta^3:\eta^3$ -manner are depicted in Figure 1.

In an  $\eta^1:\eta^1$ -complex, each metal center is  $\sigma$ -bonded to each allyl fragment.  $\eta^3:\eta^3$ -TME compounds contain two metal

### Scheme 1. Synthesis of Complexes 1–7



centers  $\pi$ -bonded to each allyl fragment. Structural data for these known complexes confirm the planarity of the ligand<sup>15,16</sup> and agree with calculations that demonstrate the complete delocalization of the  $\pi$ -electrons across the carbon skeleton, which should promote effective communication between the metal centers. However, no studies of such metal–metal interactions have yet been performed.

The most common method for the synthesis of TME complexes is to combine reactive metal fragments, i.e., photolyzed carbonyl  $\text{M}(\text{CO})_6$ , with allene,<sup>16–19</sup> but poor yields are obtained ( $< 20\%$ ) and it is not possible to synthesize more complex systems. Given the limitations of this synthetic approach, we have investigated the use of the TME precursor dipotassium 2,3-bis(methylene)-1,3-butanediyl, also referred to as potassium tetramethyleneethane (TMEK<sub>2</sub>). TMEK<sub>2</sub> can be seen as a six- $\pi$ -electron donor to one metal center or a pair of three- $\pi$ -electron donors in a homobimetallic complex, sharing the  $\pi$ -density equally between the metals. Several authors have investigated the potential of using TMEK<sub>2</sub> in organic chemistry with various electrophilic reagents, and this has been met with considerable success.<sup>20</sup> Despite this, no studies describing the direct combination of TMEK<sub>2</sub> with metal precursors has been published.

Since  $(\text{C}_3\text{H}_5)\text{Br}$  has been widely used for the synthesis of many important organometallic complexes such as  $(\pi\text{-C}_3\text{H}_5)\text{Co}(\text{CO})_3$ ,<sup>21</sup> 2,3-bis(bromomethyl)-1,3-butadiene (TMEBr<sub>2</sub>) was also chosen as a synthon. In this paper we report the synthesis and characterization of bimetallic TME complexes containing the “ $\text{Co}(\text{CO})_3$ ” and “ $\text{CoCp}^*$ ” ( $\text{Cp}^* = \eta^5\text{-C}_5\text{Me}_5$ ) metal fragments. The structural and redox properties of these

(7) Bonneman, H.; Grard, C.; Kopp, W.; Pump, W.; Tanaka, K.; Wilke, G. *Angew. Chem., Int. Ed. Engl.* **1973**, *12*, 964.

(8) Becconsa, J. K.; Job, B. E.; O'Brien, S. *J. Chem. Soc.* **1967**, 423.

(9) (a) Heck, R. F.; Breslow, D. S. *J. Am. Chem. Soc.* **1960**, *82*, 750. (b) McClellan, W.; Muettterties, E. L.; Howk, B. W.; Hoehn, H. H.; Cripps, H. N. *J. Am. Chem. Soc.* **1961**, *83*, 1601.

(10) Brown, C. K.; Mowat, W.; Yagupsky, G.; Wilkinson, G. *J. Chem. Soc.* **1971**, 850.

(11) (a) Bencini, A.; Ciofini, I.; Daul, C. A.; Ferretti, A. *J. Am. Chem. Soc.* **1999**, *121*, 11418. (b) Esponda, E.; Adams, C.; Burgos, F.; Chavez, I.; Manriquez, J. M.; Delpech, F.; Castel, A.; Gornitzka, H.; Riviere-Baudet, M.; Riviere, P. *J. Organomet. Chem.* **2006**, *691*, 3011. (c) Ferretti, A.; Lami, A.; Villani, G. *J. Phys. Chem. A* **1997**, *101*, 9439. (d) Long, N. *J. Angew. Chem., Int. Ed. Engl.* **1995**, *34*, 21. (e) Santi, S.; Cecon, A.; Bisello, A.; Durante, C.; Ganis, P.; Orian, L.; Benetollo, F.; Crociani, L. *Organometallics* **2005**, *24*, 4691. (f) Santi, S.; Orian, L.; Donoli, A.; Durante, C.; Bisello, A.; Ganis, P.; Cecon, A.; Crociani, L.; Benetollo, F. *Organometallics* **2007**, *26*, 5867. (g) Ward, M. D. *Chem. Soc. Rev.* **1995**, *24*, 121.

(12) (a) Balzani, V.; Juris, A.; Venturi, M.; Campagna, S.; Serroni, S. *Chem. Rev. (Washington, DC, U. S.)* **1996**, *96*, 759. (b) Belsler, P.; Bernhard, S.; Blum, C.; Beyeler, A.; De Cola, L.; Balzani, V. *Coord. Chem. Rev.* **1999**, *192*, 155. (c) De Cola, L.; Belsler, P. *Coord. Chem. Rev.* **1998**, *177*, 301. (d) Low, P. J.; Roberts, R. L.; Cordiner, R. L.; Hartl, F. *J. Solid State Electrochem.* **2005**, *9*, 717. (e) Newton, M. D. *Chem. Rev. (Washington, DC, U. S.)* **1991**, *91*, 767. (f) Paul, F.; Lapinte, C. *Coord. Chem. Rev.* **1998**, *178*, 431. (g) Sarkar, B.; Laye, R. H.; Mondal, B.; Chakraborty, S.; Paul, R. L.; Jeffery, J. C.; Puranik, V. G.; Ward, M. D.; Lahiri, G. K. *J. Chem. Soc., Dalton Trans.* **2002**, 2097.

(13) Bates, R. B.; Gordon, B.; Highsmith, T. K.; White, J. J. *J. Org. Chem.* **1984**, *49*, 2981.

(14) Mills, N. S.; Rusinko, A. R. *J. Org. Chem.* **1986**, *51*, 2567.

(15) Keim, W. *Angew. Chem., Int. Ed. Engl.* **1968**, *7*, 879.

(16) Lin, W. B.; Wilson, S. R.; Girolami, G. S. *Organometallics* **1997**, *16*, 2356.

(17) Leyendecker, M.; Kreiter, C. G. *J. Organomet. Chem.* **1984**, *260*, C67.

(18) Kerber, R. C.; Miran, M. J.; Waldbaum, B.; Rheingold, A. L. *Organometallics* **1995**, *14*, 2002.

(19) (a) Arce, A. J.; Chierotti, M.; De Sanctis, Y.; Deeming, A. J.; Gobetto, R. *Inorg. Chim. Acta* **2004**, *357*, 3799. (b) Kreiter, C. G.; Kogler, J.; Nist, K. *J. Organomet. Chem.* **1986**, *310*, 35.

(20) (a) Bates, R. B.; Gordon, B.; Highsmith, T. K.; White, J. J. *J. Org. Chem.* **1984**, *49*, 2981. (b) Gordon, B.; Blumenthal, M. *Polym. Bull. (Berlin, Germany)* **1985**, *14*, 69.

(21) (a) Harvey, M. J.; Hanusa, T. P.; Young, V. G. *Angew. Chem., Int. Ed.* **1999**, *38*, 217. (b) Smith, J. D.; Hanusa, T. P.; Young, V. G. *J. Am. Chem. Soc.* **2001**, *123*, 6455.

new complexes are also discussed. We also report several ligand exchange reactions performed with the  $\text{TME}[\text{Co}(\text{CO})_3]_2$  (**1**) system.

## Results and Discussion

**Synthesis and Characterization.** As depicted in Scheme 1, the dicobalt complex ( $\eta^3:\eta^3$ -TME)[Co(CO)<sub>3</sub>]<sub>2</sub> (**1**) was readily obtained by reaction of  $\text{TMEBr}_2$  with 2 equiv of  $\text{Na}[\text{Co}(\text{CO})_4]$  at  $-80^\circ\text{C}$ . The orange-yellow product was purified by recrystallization from toluene. It is soluble in toluene, hexane, MeCN, and  $\text{CH}_2\text{Cl}_2$ . However, **1** appears to react with MeCN at room temperature when exposed to sunlight (change of color), presumably due to a ligand exchange reaction occurring between the carbonyl group and MeCN. This type of reaction has been observed on complexes containing the  $\text{Fe}(\text{CO})_3$  fragment, under similar conditions.<sup>22</sup> The family of complexes ( $\eta^3:\eta^3$ -TME)[Co(CO)<sub>2</sub>PR<sub>3</sub>]<sub>2</sub> (R = Me, **2**; Et, **3**; *n*-Bu, **4**; Ph, **5**; OPh, **6**) were obtained by the reaction of **1** with an excess of the corresponding phosphine precursor, where only one CO is exchanged. The orange-yellow solids were purified by recrystallization from hydrocarbon or a mixture of hydrocarbon/aromatic solvents. All these complexes are slightly air-sensitive as a solid and in solution, but are stable for months under an atmosphere of nitrogen.

The synthesis of  $\text{TMEK}_2$  was optimized to high yield (80–85%) using KO*t*-Am (*Ot*-Am = 1,1-dimethylpropoxide) instead of KO*t*-Bu, which is highly soluble in the hydrocarbon solvent, used for deprotonation. Furthermore, the byproduct Li*Ot*-Am can be easily removed from the dipotassium salt by several washings with hexane.

The metathesis reaction of  $\text{Cp}^*\text{Co}(\text{acac})$  with  $\text{TMEK}_2$  yielded ( $\eta^4:\eta^4$ -TME)[CoCp\*]<sub>2</sub> (**7**) through salt elimination. **7** is a deep purple, air-sensitive solid that can be kept for months under an atmosphere of nitrogen. It is soluble in toluene, hexane,  $\text{CH}_2\text{Cl}_2$ , and MeCN. The  $\eta^4:\eta^4$ -configuration was confirmed by X-ray diffraction (Figure 6). This was unexpected, as all previously known TME complexes exhibit either an  $\eta^1:\eta^1$ - or an  $\eta^3:\eta^3$ -configuration, with the TME ligand acting as a one- $\pi$ -electron or three- $\pi$ -electron donor to each metal center, respectively. In **7**, the TME fragment is acting as a four- $\pi$ -electron donor to each metal center when it is formally only a six- $\pi$ -electron donor ligand, giving a 34-electron complex. The electron counting is nontrivial, as the two Co centers share the electrons of the two central carbon atoms from the TME unit. The phenomenon of sharing electrons from the same carbon atoms within metal centers is commonly seen in triple-decker complexes.<sup>23</sup> The interesting  $\eta^4:\eta^4$ -configuration was also observed in the triple-decker complex ( $\mu$ - $\eta^4:\eta^4$ -arene)[CoCp\*]<sub>2</sub>. The electron count for this complex is also 34.<sup>24</sup>

In 1976, Hoffmann et al.<sup>25</sup> predicted two series of stable triple-decker complexes (based on CpM–Cp–MCp) with a 30- and 34-electron rule, in analogy to the 18-electron rule for metallocenes. Even though complexes ( $\mu$ - $\eta^4:\eta^4$ -C<sub>6</sub>H<sub>5</sub>*i*-Pr)[CoCp\*]<sub>2</sub> and **7** are not “true” triple-decker compounds, as the metals do not bind to all of the carbon atoms of the

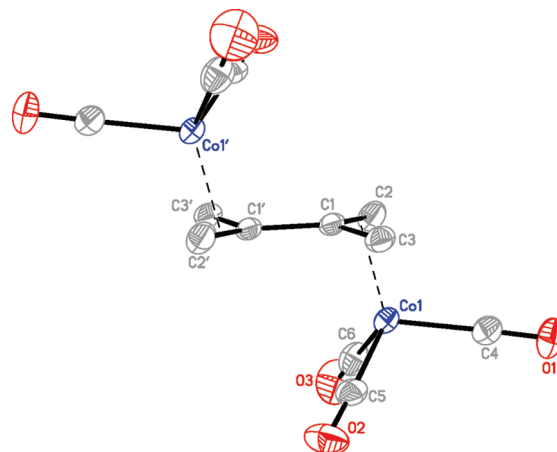


**Figure 2.** Molecular structure of **1** from single-crystal diffraction data. Hydrogen atoms are omitted for clarity, and displacement ellipsoids are drawn at 50% probability. Primed atoms are generated by  $-x, -y, -z$ .

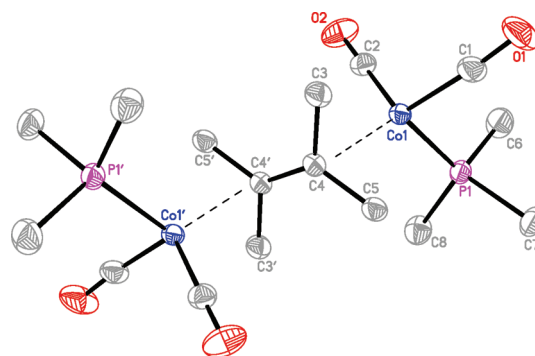


**Figure 3.** Molecular structure of **2** from single-crystal diffraction data. Hydrogen atoms are omitted for clarity, and displacement ellipsoids are drawn at 50% probability. Primed atoms are generated by  $-x, -y, -z$ .

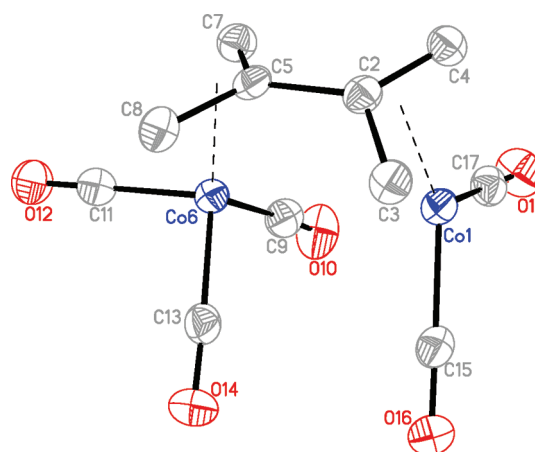


**Figure 4.** Molecular structure of the decomposition product of **1**<sup>+</sup> (**1**<sup>d</sup>). Hydrogen atoms and the  $[\text{BF}_4]^-$  anion have been omitted for clarity, and displacement ellipsoids are at 50%.

central structure (arene and TME ligands, respectively), they do obey the 30- and 34-electron rule of Hoffmann.<sup>23</sup>

Attempts to oxidize complexes **1**, **2**, **3**, and **7** were performed using  $\text{AgBF}_4$  as an oxidizing agent. This reaction was

(22) Knölker, H. J.; Goesmann, H.; Klaus, R. *Angew. Chem., Int. Ed.* **1999**, *38*, 702.

(23) Beck, V.; O'Hare, D. *J. Organomet. Chem.* **2004**, *689*, 3920.

(24) Schneider, J. J.; Denninger, U.; Heinemann, O.; Kruger, C. *Angew. Chem., Int. Ed. Engl.* **1995**, *34*, 592.

(25) Lauher, J. W.; Elian, M.; Summerville, R. H.; Hoffmann, R. *J. Am. Chem. Soc.* **1976**, *98*, 3219.

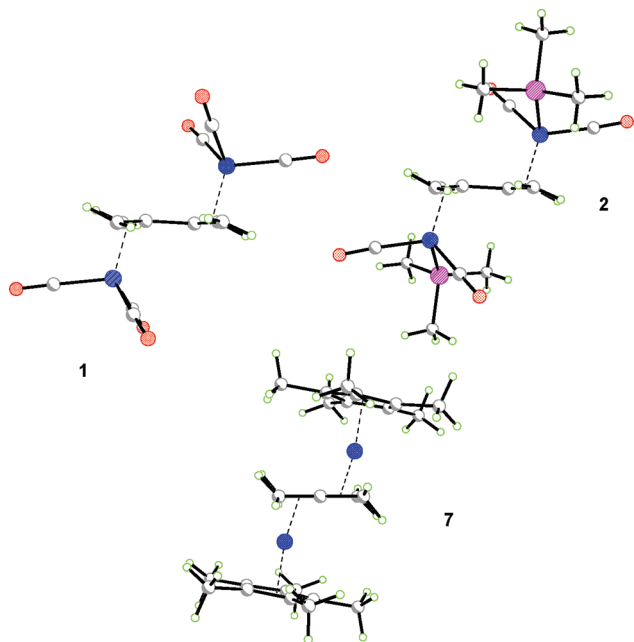


**Figure 5.** Compounds **1**, **2**, and **7** showing the hydrogen displacement from the TME plane.

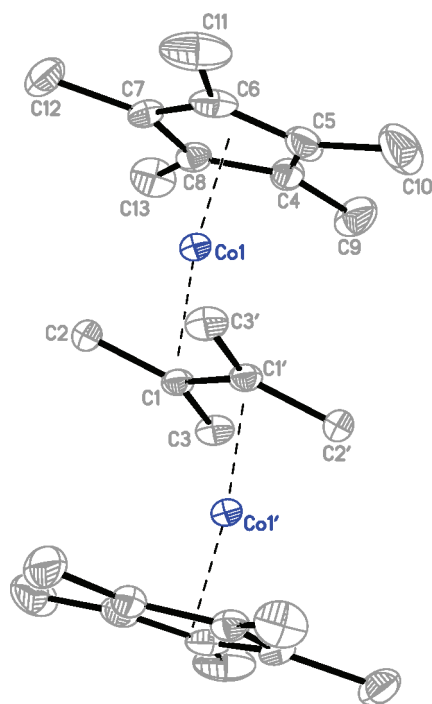
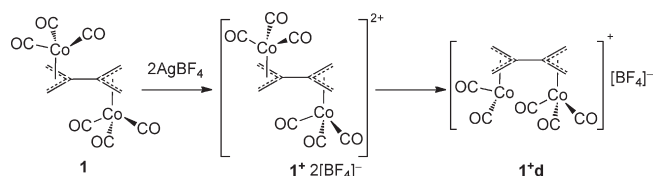


**Figure 6.** Molecular structure of **7** from single-crystal diffraction data. Hydrogen atoms are omitted for clarity, and displacement ellipsoids are drawn at 50% probability.

successful only for **1**, where a solid was isolated that was consistent with the formula  $\{\text{TME}[\text{Co}(\text{CO})_3]_2\}^{2+}[\text{BF}_4]^{-}_2$  (**1**<sup>+</sup>) given by elemental analysis. This solid appeared to be very unstable in  $\text{CH}_2\text{Cl}_2$  and  $\text{MeNO}_2$  solutions, decomposing after approximately one hour. The instability of **1**<sup>+</sup> can be seen in the decomposition product obtained from a solution of **1**<sup>+</sup>:  $\{[(\text{CO})_2\text{Co}]\text{TME}[\text{Co}(\text{CO})_3]\}^+[\text{BF}_4]^-$  (**1**<sup>+</sup>**d**) (Scheme 2).

The identity of all the products was established by elemental analysis, mass spectroscopy, <sup>1</sup>H and <sup>13</sup>C NMR, IR spectroscopy

### Scheme 2. Formation of **1**<sup>+</sup> and Decomposition Product **1**<sup>+</sup>**d**



copy (except **7**), cyclic voltammetry (CV), and single-crystal X-ray diffraction; the results are given below.

**<sup>1</sup>H and <sup>13</sup>C NMR Spectroscopy.** Table 1 summarizes the NMR spectroscopic data for all complexes. <sup>1</sup>H NMR spectroscopy of the diamagnetic complexes **1–6** showed resonances for the TME fragment in a 1:1 ratio, which is consistent with the metal centers bound in an  $\eta^3:\eta^3$ -configuration and is also consistent with that reported for  $(\eta^3\text{-C}_3\text{H}_5)\text{Co}(\text{CO})_3$ . The latter showed three sets of resonances in a 1:2:2 ratio with a symmetrical structure. The hydrogen atom of the central carbon atom appeared at 4.91 ppm as a multiplet, while the *syn*- and *anti*-hydrogens of the terminal carbon atom of the allyl group appeared as a pair of doublets at 3.06 and 2.15 ppm, with the splitting due to the hydrogen atom of the central carbon atom of the allyl group. <sup>13</sup>C NMR spectroscopy was comparable with that reported for  $(\eta^3\text{-C}_3\text{H}_5)\text{Co}(\text{CO})_3$ .<sup>21</sup> The spectra of **7** also displayed resonances for the TME fragment in a 1:1 ratio, consistent with a symmetrical structure, although the crystal structure showed an  $\eta^4:\eta^4$ -configuration.

**IR Spectroscopy.** IR spectroscopy was used to study the carbonyl vibrations in the family of complexes **1–6** and to determine the effect of the different phosphine groups on these vibrations.  $(\pi\text{-C}_3\text{H}_5)\text{Co}(\text{CO})_3$  is expected to have two IR-active vibrations for the carbonyl group ( $A_1$  and  $E$ ) if the local symmetry is taken into account ( $C_{3v}$ ) and three IR-active vibrations ( $2A'$  and  $A''$ ) if the overall symmetry is considered ( $C_s$ ). It has been shown elsewhere that the use of the former treatment to assign carbonyl frequencies is adequate.<sup>26</sup> Hence, the IR studies of the complexes herein will only consider local symmetries. The local symmetry of the  $\text{Co}(\text{CO})_2\text{PR}_3$  fragment is  $C_s$ ; consequently complexes **2–6** should present two IR-active vibrations for the carbonyl group ( $A'$  and  $A''$ ). Since the local symmetry of the  $\text{Co}(\text{CO})_3$  fragment is  $C_{3v}$ , **1** should present two IR-active vibrations for the carbonyl group ( $A_1$  and  $E$ ).<sup>26b,27</sup> The IR spectra recorded (KBr disk) display two bands characteristic of carbonyl stretchings; these are summarized in Table 2.

As expected, the vibrations observed for the carbonyl groups for **1** are shifted to lower frequencies when one of the carbonyl groups is exchanged for a phosphine group on each metal center. The extent of the shift is influenced by the substitution on the phosphine group, since this affects its donor property. The ordering of the  $\text{PR}_3$  groups according to their electron-donating properties should be  $\text{PEt}_3 > \text{P}n\text{-Bu}_3 > \text{PMe}_3 > \text{PPh}_3 > \text{P}(\text{O}i\text{Pr})_3$ . The IR frequencies found in this family of complexes tend to agree with this trend. The values found for **2**, **4**, and **5** are close, suggesting that the electron-donating properties of  $\text{PMe}_3$ ,  $\text{P}n\text{-Bu}_3$ , and  $\text{PPh}_3$  groups are very similar. The IR spectrum of **6** shows two vibrations for the carbonyl

(26) (a) Andrews, D. C.; Davidson, G. *J. Chem. Soc., Dalton Trans.* **1972**, 1381. (b) Paliani, G.; Murgia, S. M.; Cardaci, G.; Cataliotti, R. *J. Organomet. Chem.* **1973**, *63*, 407. (c) Yurchenko, E. N. *J. Struct. Chem.* **1977**, *18*, 399.

(27) Paliani, G.; Poletti, A.; Cardaci, G.; Murgia, S. M.; Cataliotti, R. *J. Organomet. Chem.* **1973**, *60*, 157.

Table 1. Summary of the  $^1\text{H}$  and  $^{13}\text{C}$  NMR Spectroscopic Data for 1–7<sup>a</sup>

complex	$^1\text{H}$ resonances			$^{13}\text{C}$ resonances				
	<i>syn</i> -H	<i>anti</i> -H	Cp*H	C <sub>Term</sub>	C <sub>Cent</sub>	CpC	CpMe	CO
( $\eta^3$ : $\eta^3$ -TME)[Co(CO) <sub>3</sub> ] <sub>2</sub> , <b>1</b>	2.85	1.36		45.10	98.21			202.75
( $\eta^3$ : $\eta^3$ -TME)[Co(CO) <sub>2</sub> PMe <sub>3</sub> ] <sub>2</sub> , <b>2</b>	2.79	1.54		39.35	98.14			205.1
( $\eta^3$ : $\eta^3$ -TME)[Co(CO) <sub>2</sub> PEt <sub>3</sub> ] <sub>2</sub> , <b>3</b>	2.83	1.58		38.81	98.33			205.90
( $\eta^3$ : $\eta^3$ -TME)[Co(CO) <sub>2</sub> <i>Pn</i> -Bu <sub>3</sub> ] <sub>2</sub> , <b>4</b>	3.02	1.74		39.02	98.84			206.13
( $\eta^3$ : $\eta^3$ -TME)[Co(CO) <sub>2</sub> PPh <sub>3</sub> ] <sub>2</sub> , <b>5</b>	2.89	1.44		43.28	99.15			206.13
( $\eta^3$ : $\eta^3$ -TME)[Co(CO) <sub>2</sub> P(OPh) <sub>3</sub> ] <sub>2</sub> , <b>6</b>	3.16	1.63		43.66	97.75			205.05
( $\eta^4$ : $\eta^4$ -TME)[CoCp*] <sub>2</sub> , <b>7</b>	1.77	−0.44	1.71	26.87	69.67	89.18	10.15	

<sup>a</sup> Multiplicity of resonances and *J* values are given in the Experimental Section.

Table 2. Summary of the Carbonyl Stretching Frequencies for 1–6

complex	$\nu(\text{CO})$	$\nu(\text{CO})$	ref
( $\eta^3$ : $\eta^3$ -TME)[Co(CO) <sub>3</sub> ] <sub>2</sub> , <b>1</b> <sup>a</sup>	2053 (A <sub>1</sub> )	1985 (E)	this work
( $\eta^3$ -C <sub>3</sub> H <sub>5</sub> )Co(CO) <sub>3</sub> <sup>a</sup>	2062 (A <sub>1</sub> )	1980 (E)	26b
( $\eta^3$ : $\eta^3$ -TME)[Co(CO) <sub>2</sub> PMe <sub>3</sub> ] <sub>2</sub> , <b>2</b> <sup>a</sup>	1968 (A')	1917 (A')	this work
( $\eta^3$ : $\eta^3$ -TME)[Co(CO) <sub>2</sub> PEt <sub>3</sub> ] <sub>2</sub> , <b>3</b> <sup>a</sup>	1957 (A')	1920 (A')	this work
( $\eta^3$ -C <sub>3</sub> H <sub>5</sub> )Co(CO) <sub>2</sub> PEt <sub>3</sub> <sup>b</sup>	1990 (A')	1930 (A')	28
( $\eta^3$ : $\eta^3$ -TME)[Co(CO) <sub>2</sub> <i>Pn</i> -Bu <sub>3</sub> ] <sub>2</sub> , <b>4</b> <sup>a</sup>	1972 (A')	1912 (A')	this work
( $\eta^3$ -C <sub>3</sub> H <sub>5</sub> )Co(CO) <sub>2</sub> <i>Pn</i> -Bu <sub>3</sub> <sup>a</sup>	1973 (A')	1912 (A')	29
( $\eta^3$ : $\eta^3$ -TME)[Co(CO) <sub>2</sub> PPh <sub>3</sub> ] <sub>2</sub> , <b>5</b> <sup>a</sup>	1974 (A')	1918 (A')	this work
( $\eta^3$ -C <sub>3</sub> H <sub>5</sub> )Co(CO) <sub>2</sub> PPh <sub>3</sub> <sup>c</sup>	1985 (A')	1928 (A')	29
( $\eta^3$ : $\eta^3$ -TME)[Co(CO) <sub>2</sub> P(OPh) <sub>3</sub> ] <sub>2</sub> , <b>6</b> <sup>a</sup>	2009 (A')	1962 (A'), 1969 (asymmetry)	this work
( $\eta^3$ -C <sub>3</sub> H <sub>5</sub> )Co(CO) <sub>2</sub> P(OPh) <sub>3</sub> <sup>c</sup>	2019 (A')	1974 (A'), 1984 (asymmetry)	30

<sup>a</sup> KBr disk. <sup>b</sup> Pentane. <sup>c</sup> Cyclohexane.

groups.  $\nu(\text{CO})$  A'' presents an asymmetry on the main band at 1969 cm<sup>−1</sup>. The IR spectrum of ( $\eta^3$ -C<sub>3</sub>H<sub>5</sub>)Co(CO)<sub>2</sub>P(OPh)<sub>3</sub> displays two vibrations for the carbonyl groups at 2019 and 1974 cm<sup>−1</sup>. This last vibration also presents an asymmetry of the main band at 1984 cm<sup>−1</sup>.<sup>30</sup>

**Electrochemical Properties.** The electrochemical properties of **1–7** were measured by cyclic voltammetry in MeCN (**1–6**) and CH<sub>2</sub>Cl<sub>2</sub> (**7**) solutions containing 0.1 M [*n*-Bu<sub>4</sub>N]<sup>+</sup>[BF<sub>4</sub>]<sup>−</sup>. The cyclic voltammograms recorded for each complex exhibited two electrochemical events believed to correspond to the oxidation of the cobalt centers and suggests that the oxidation of one metal center affects the oxidation potential of the second.

Table 3 summarizes the electrochemical data for this series of complexes. The couples involved are believed to be Co<sup>II</sup>Co<sup>II</sup>/Co<sup>II</sup>Co<sup>I</sup> and Co<sup>II</sup>Co<sup>I</sup>/Co<sup>I</sup>Co<sup>I</sup> for complexes **1–6** and Co<sup>III</sup>Co<sup>III</sup>/Co<sup>III</sup>Co<sup>II</sup> and Co<sup>III</sup>Co<sup>II</sup>/Co<sup>II</sup>Co<sup>II</sup> for **7**. Previous electrochemical studies on the mononuclear species ( $\pi$ -C<sub>3</sub>H<sub>5</sub>)Co(CO)<sub>3</sub> show a two-electron irreversible process at  $E_{1/2} = -2.00$  V (referenced to [Cp<sub>2</sub>Fe]<sup>+</sup>/Cp<sub>2</sub>Fe) that corresponds to the double reduction of the complex, resulting in decomposition and the formation of [Co(CO)<sub>4</sub>]<sup>−</sup>.<sup>29</sup> No oxidation processes have been reported. Since the processes observed for **1–6** appear at much more positive potentials compared to ( $\eta^3$ -C<sub>3</sub>H<sub>5</sub>)Co(CO)<sub>3</sub>, we believe them to be oxidation processes.

The separation of the two electrochemical events,  $\Delta E$  ( $E_2 - E_1$ ), may be used as a measure of the electronic stabilization imparted on the mixed valence species by the second metal center in the molecule and thus regarded as a measure

Table 3. Summary of the Electrochemical Data for 1–7<sup>a</sup>

complex	$E_1$ (V)	$E_2$ (V)	$\Delta E$ (mV)
( $\eta^3$ : $\eta^3$ -TME)[Co(CO) <sub>3</sub> ] <sub>2</sub> , <b>1</b>	+0.25 <sup>b</sup>	+0.50 <sup>b</sup>	250
( $\eta^3$ : $\eta^3$ -TME)[Co(CO) <sub>2</sub> PMe <sub>3</sub> ] <sub>2</sub> , <b>2</b>	−0.07 <sup>b</sup>	+0.15 <sup>b</sup>	220
( $\eta^3$ : $\eta^3$ -TME)[Co(CO) <sub>2</sub> PEt <sub>3</sub> ] <sub>2</sub> , <b>3</b>	−0.27 <sup>b</sup>	+0.03 <sup>b</sup>	300
( $\eta^3$ : $\eta^3$ -TME)[Co(CO) <sub>2</sub> <i>Pn</i> -Bu <sub>3</sub> ] <sub>2</sub> , <b>4</b>	−0.21 <sup>b</sup>	+0.07 <sup>b</sup>	280
( $\eta^3$ : $\eta^3$ -TME)[Co(CO) <sub>2</sub> PPh <sub>3</sub> ] <sub>2</sub> , <b>5</b>	−0.03 <sup>b</sup>	+0.39 <sup>c</sup>	
( $\eta^3$ : $\eta^3$ -TME)[Co(CO) <sub>2</sub> P(OPh) <sub>3</sub> ] <sub>2</sub> , <b>6</b>	−0.05 <sup>b</sup>	+0.36 <sup>c</sup>	
( $\eta^4$ : $\eta^4$ -TME)[CoCp*] <sub>2</sub> , <b>7</b>	−0.91 <sup>d</sup>	−0.47 <sup>c</sup>	

<sup>a</sup> All redox potentials are relative to the couple [Cp<sub>2</sub>Fe]<sup>+</sup>/Cp<sub>2</sub>Fe. <sup>b</sup> Quasi-reversible. <sup>c</sup> Irreversible oxidation. <sup>d</sup> Reversible.

of the electronic delocalization mediated by the ligand.<sup>31</sup> Complexes **1–4** display significant electronic interaction between the metal centers, whereas for complexes **5–7**, it is not possible to calculate  $\Delta E$ , as these systems present irreversible oxidations.

The electron-donating properties of the PR<sub>3</sub> fragments increase the electron density on the metal center, and as expected, this produces shifts of  $E_1$  and  $E_2$  to more cathodic potentials relative to **1**; for this family of complexes, both oxidations are easier to achieve. In addition PR<sub>3</sub> incorporation stabilizes the oxidized species, as seen by the greater  $\Delta E$  values. The greatest electron donation was observed when PEt<sub>3</sub> was used (both couples were shifted to more cathodic potentials relative to **1**, **2**, **5**, and **6**, and the system displayed significant electronic communication between the metal centers). The lowest degree of electron donation was observed for **5** and **6**, where the oxidized species are less stable than those of **2–4**. The redox couple observed for **6** is shifted to more cathodic potentials compared to **5**. One possible cause of this is the presence of the O atoms, which increase the electron density of the P(OPh)<sub>3</sub> group relative to PPh<sub>3</sub>. Similarly to that observed in the IR spectroscopy studies, the effect of the electron-donating properties on the redox potentials followed the trend PEt<sub>3</sub> > *Pn*-Bu<sub>3</sub> > PMe<sub>3</sub> > PPh<sub>3</sub> ≈ P(OPh)<sub>3</sub>.

(28) Dickson, R. S.; Yin, P.; Ke, M.; Johnson, J.; Deacon, G. B. *Polyhedron* **1996**, *15*, 2237.

(29) Cardaci, G.; Murgia, S. M.; Paliani, G. *J. Organomet. Chem.* **1974**, *77*, 253.

(30) Clarke, H. L.; Fitzpatrick, N. J. *Inorg. Nucl. Chem. Lett.* **1973**, *9*, 75.

(31) Barlow, S.; O'Hare, D. *Chem. Rev. (Washington, DC, U. S.)* **1997**, *97*, 637.

**Table 4.** Details of Crystal Structure Parameters and Refinements for Complexes **1–7** and **1<sup>+</sup>d**

	<b>1</b>	<b>1<sup>+</sup>d</b>	<b>2</b>	<b>3</b>	<b>4</b>	<b>5</b>	<b>6</b>	<b>7</b>
formula	C <sub>12</sub> H <sub>8</sub> Co <sub>2</sub>	C <sub>11</sub> H <sub>8</sub> BCo <sub>2</sub> <sup>-</sup> F <sub>4</sub> O <sub>5</sub>	C <sub>16</sub> H <sub>26</sub> Co <sub>2</sub> <sup>-</sup> O <sub>4</sub> P <sub>2</sub>	C <sub>22</sub> H <sub>38</sub> Co <sub>2</sub> <sup>-</sup> O <sub>4</sub> P <sub>2</sub>	C <sub>34</sub> H <sub>62</sub> Co <sub>2</sub> <sup>-</sup> O <sub>4</sub> P <sub>2</sub>	C <sub>46</sub> H <sub>38</sub> Co <sub>2</sub> <sup>-</sup> O <sub>4</sub> P <sub>2</sub>	C <sub>46</sub> H <sub>38</sub> Co <sub>2</sub> <sup>-</sup> O <sub>10</sub> P <sub>2</sub>	C <sub>26</sub> H <sub>38</sub> Co <sub>2</sub>
fw	366.06	424.85	462.17	546.35	714.64	834.56	930.56	468.45
size/mm	0.18, 0.22, 0.22	0.15, 0.13, 0.09	0.2, 0.06, 0.04	0.12, 0.12, 0.28	0.06, 0.04, 0.02	0.2, 0.06, 0.04	0.22, 0.18, 0.1	0.06, 0.2, 0.24
cryst class	triclinic	orthorhombic	triclinic	monoclinic	triclinic	triclinic	monoclinic	monoclinic
space group	P $\bar{1}$	P 2 <sub>1</sub> 2 <sub>1</sub> 2 <sub>1</sub>	P $\bar{1}$	P $\bar{1}$	P $\bar{1}$	P $\bar{1}$	P2 <sub>1</sub> /c	P2 <sub>1</sub> /c
<i>a</i> /Å	6.6398(2)	7.4109(2)	6.8755(2)	6.9927(2)	9.7293(2)	9.4902(2)	9.4540(1)	9.5675(3)
<i>b</i> /Å	6.7052(2)	12.9909(3)	8.7561(3)	14.0728(2)	9.7312(2)	9.5480(2)	18.3056(3)	14.2717(5)
<i>c</i> /Å	8.1460(3)	15.0675(4)	8.9500(2)	13.3788(2)	10.5514(3)	10.3123(2)	12.1477(2)	9.9283(3)
$\alpha$ /deg	88.3649(14)	90	87.994(2)	90	93.519(1)	92.954(1)	90	90
$\beta$ /deg	78.8043(14)	90	75.764(2)	101.2813(5)	102.906(1)	95.132(1)	95.761(1)	101.8273(12)
$\gamma$ /deg	76.2844(16)	90	85.0410(10)	90	101.6571(1)	95.769(1)	90	90
<i>V</i> /Å <sup>3</sup>	345.56(2)	1450.61(6)	520.26(3)	1291.13(5)	947.71(4)	924.23(3)	2091.68(5)	1131.71(7)
<i>Z</i>	1	4	1	2	1	1	2	2
$\rho_c$ /g cm <sup>-3</sup>	1.759	1.945	0.475	0.405	1.252	1.499	1.478	1.375
<i>F</i> (000)	182	836	238	572	382	430	956	496
$\mu$ /mm <sup>-1</sup>	2.419	2.351	1.763	1.432	0.992	1.030	0.929	1.474
$\theta$ range/deg	5.0–27.5	5.13–27.43	4.26–27.44	5–27.5	3.99–27.09	5.15–28.64	3.98–27.47	5–27.5
total no. of data	4237	22 999	3731	13 136	7260	15 279	9185	10 378
no. of unique data	1574 <i>R</i> <sub>(int)</sub> = 0.023	3315 <i>R</i> <sub>(int)</sub> = 0.051	2316 <i>R</i> <sub>(int)</sub> = 0.022	3055 <i>R</i> <sub>(int)</sub> = 0.022	4148 <i>R</i> <sub>(int)</sub> = 0.053	4365 <i>R</i> <sub>(int)</sub> = 0.045	4767 <i>R</i> <sub>(int)</sub> = 0.024	2681 <i>R</i> <sub>(int)</sub> = 0.027
no. obsd reflns	1377 <sup>a</sup>	3034 <sup>b</sup>	2192 <sup>b</sup>	2564 <sup>a</sup>	3193 <sup>b</sup>	4102 <sup>b</sup>	4480 <sup>b</sup>	1911 <sup>a</sup>
GOF	1.1439	1.0873	1.050	1.0828	1.012	1.030	1.019	1.0238
<i>R</i> indices	<i>R</i> <sub>1</sub> = 0.0242 <i>wR</i> <sub>2</sub> = 0.0252	<i>R</i> <sub>1</sub> = 0.0321 <i>wR</i> <sub>2</sub> = 0.0282	<i>R</i> <sub>1</sub> = 0.0367 <i>wR</i> <sub>2</sub> = 0.0650	<i>R</i> <sub>1</sub> = 0.0229 <i>wR</i> <sub>2</sub> = 0.0249	<i>R</i> <sub>1</sub> = 0.0818 <i>wR</i> <sub>2</sub> = 0.1003	<i>R</i> <sub>1</sub> = 0.0579 <i>wR</i> <sub>2</sub> = 0.0833	<i>R</i> <sub>1</sub> = 0.0541 <i>wR</i> <sub>2</sub> = 0.0826	<i>R</i> <sub>1</sub> = 0.0294 <i>wR</i> <sub>2</sub> = 0.0369
residuals/e Å <sup>-3</sup>	-0.33, 0.36	-0.31, 0.38	-0.35, 0.37	-0.25, 0.33	-0.43, 0.53	-0.42, 0.48	-0.31, 0.23	-0.45, 0.59

<sup>a</sup> *I* > 3 $\sigma$ (*I*). <sup>b</sup> *I* > 2 $\sigma$ (*I*).**Table 5a.** Selected Bond Lengths (Å) for Complexes **1–7** and **1<sup>+</sup>d**

	<b>1</b>	<b>1<sup>+</sup>d</b>	<b>2</b>	<b>3</b>	<b>4</b>	<b>5</b>	<b>6</b>	<b>7</b>
Co–C(CO)	1.818(2) 1.780(2)	1.817(3) <sup>a</sup> 1.839(3) <sup>a</sup> 1.798(3) <sup>b</sup> 1.845(3) <sup>b</sup> 1.803(3) <sup>b</sup>	1.770(2) 1.759(2)	1.7790(15) 1.7559(15)	1.773(3) 1.743(3)	1.791(2) 1.739(2)	1.771(2) 1.766(2)	
Co–C <sub>Term</sub>	2.092(2) 2.0796(12)	2.068(3) <sup>a</sup> 2.088(3) <sup>a</sup> 2.088(3) <sup>b</sup> 2.111(3) <sup>b</sup> 2.027(2) <sup>a</sup> 2.020(2) <sup>b</sup>	2.061(2) 2.1006(19)	2.0641(14) 2.1045(15)	2.054(3) 2.098(3)	2.035(2) 2.095(2)	2.068(2) 2.0770(19)	2.0109(18) 2.0086(19)
Co–C <sub>Cent</sub>	2.0173(17)	2.027(2) <sup>a</sup> 2.020(2) <sup>b</sup>	2.0257(19)	2.0338(13)	2.023(3)	2.0349(19)	2.0097(17)	2.0124(17) 2.0116(17)
C <sub>Cent</sub> –C <sub>Cent</sub>	1.488(4)	1.498(3)	1.485(3)	1.489(3)	1.484(5)	1.471(4)	1.481(3)	1.546(3)
C <sub>Term</sub> –C <sub>Cent</sub>	1.414(3) 1.420(3)	1.411(3) <sup>a</sup> 1.404(3) <sup>a</sup> 1.422(4) <sup>b</sup> 1.408(4) <sup>b</sup>	1.413(3) 1.427(3)	1.429(2) 1.417(2)	1.430(4) 1.410(4)	1.358(3) 1.416(3)	1.413(3) 1.424(3)	1.453(2) 1.434(3)
Co–P			2.1692(5)	2.1902(4)	2.1811(9)	2.1318(6)	2.1594(5)	
Co–Cp*Ct								1.6698(2)
mean Co–C(cp*)								2.06(2)

<sup>a</sup> Corresponds to the Co(CO)<sub>2</sub> fragments. <sup>b</sup> Corresponds to the Co(CO)<sub>3</sub> fragments.

**Description of the Structures.** The solid-state structures of complexes **1–7** and **1<sup>+</sup>d** were determined by single-crystal X-ray diffraction. Complexes **3–6** have structures that are very similar to those of **1** and **2**, so are not discussed in great detail here.

In general, the complexes are located on a crystallographic center of inversion, which ensures the planes defined by the two allyl groups are parallel (Figures 2 and 3). For **1**, the local geometry of the Co–TME–Co core closely approximates to C<sub>2h</sub>, but the CO ligands are arranged slightly less symmetrically (due to the  $\pi$ -bonding between the metal and allyl moiety).<sup>2,5,32</sup> The hydrocarbon ligand deviates slightly from planarity such that the terminal carbon atoms (hereafter

referred to as C<sub>Term</sub>) bend slightly toward the cobalt center. This can be quantified by the deviation of the central carbon atom (hereafter referred to as C<sub>Cent</sub>) from the plane defined by the four terminal carbon atoms (0.047(2) Å).<sup>33</sup> Since the hydrocarbon moiety consists of two rigorously parallel allyl groups, it is also possible to calculate the distance between the planes (0.18(1) Å).<sup>34</sup> The cobalt atom is displaced by 1.689(1) Å along the normal to the plane defined by its coordinated allyl carbon atoms. The structure of **1** has bond

(33) The standard uncertainties for C1 are approximately isotropic, giving an error of 0.002 Å in *x*, *y*, and *z*. Assuming the error for the plane defined by the four terminal carbon atoms is negligible, this can be regarded as the error associated with the C1 deviation from the plane. All six distances (for structures **1–6**) are in the range 0.043–0.049, with errors of 0.0001–0.003, suggesting the deviation is significant. A similar approach was used to estimate the error for other distances to planes.

(32) Albright, T. A.; Hofmann, P.; Hoffmann, R. *J. Am. Chem. Soc.* **1977**, *99*, 7546.

Table 5b. Selected Bond Angles (deg) for Complexes 1–7 and 1<sup>+</sup>d

	1	1 <sup>+</sup> d	2	3	4	5	6	7
C(CO)–Co–C(CO)	97.48(10) 107.5(9) 105.14(10)	103.30(12) <sup>a</sup> 98.08(13) <sup>b</sup> 100.64(13) <sup>b</sup> 99.80(12) <sup>b</sup>	112.79(9)	110.62(7)	110.52(12)	117.96(10)	96.61(9)	
Co–C(CO)–O(CO)	176.80(17) 178.68(19)	178.5(2) <sup>a</sup> 176.4(3) <sup>a</sup> 173.3(2) <sup>b</sup> 176.7(3) <sup>b</sup> 177.7(2) <sup>b</sup>	174.66(18) 177.92(17)	173.53(15) 177.26(14)	173.4(3) 177.9(3)	176.73(19) 177.7(2)	176.16(19) 177.87(18)	
C <sub>Cent</sub> –C <sub>Cent</sub> –C <sub>Term</sub>	123.2(2) 123.3(2)	122.6(2) <sup>c</sup> 122.2(2) <sup>c</sup> 120.1(2) <sup>d</sup> 121.2(2) <sup>d</sup>	123.0(2) 123.3(2)	122.73(16) 123.08(16)	123.5(3) 123.2(3)	123.4(2) 122.4(2)	123.3(2) 123.5(2)	113.54(19) 114.77(19)
C <sub>Term</sub> –C <sub>Cent</sub> –C <sub>Term</sub>	112.96(18)	116.4(2) <sup>a</sup> 114.4(2) <sup>b</sup>	113.12(17)	113.62(13)	112.8(3)	113.5(3)	112.65(17)	131.69(17)
C(CO)–Co–P			95.70(6) 97.87(7)	100.33(5) 93.41(5)	94.71(10) 99.07(10)	97.73(7) 90.42(7)	107.58(6) 111.47(7)	
Co–P–C(alkyl)			114.50(8) 114.93(8) 117.71(7)	114.41(5) 114.06(5) 117.42(5)	117.14(9) 112.34(10) 117.22(11)	118.29(7) 114.93(7) 111.60(7)		
C(alkyl)–P–C(alkyl)			102.83(10) 102.76(10) 102.10(11)	103.54(7) 101.80(7) 103.88(7)	104.58(13) 99.65(13) 104.10(12)	106.47(9) 100.88(9) 102.61(9)		
TME Ct–Co–Cp*Ct								170.781(15) <sup>e</sup>
C <sub>Cent</sub> –Co–Cp*Ct								144.19(5)/143.69(5) <sup>e</sup>
C <sub>Term</sub> –Co–Cp*Ct								135.55(6)/134.36(6) <sup>e</sup>

<sup>a</sup> Corresponds to the Co(CO)<sub>2</sub> fragments. <sup>b</sup> Corresponds to the Co(CO)<sub>3</sub> fragments. <sup>c</sup> Corresponds to the angle between the C<sub>Cent</sub> of the Co(CO)<sub>2</sub> fragment and the C<sub>Cent</sub> and C<sub>Term</sub> of the Co(CO)<sub>3</sub> fragment. <sup>d</sup> Corresponds to the angle between the C<sub>Cent</sub> of the Co(CO)<sub>3</sub> fragment and the C<sub>Cent</sub> and C<sub>Term</sub> of the Co(CO)<sub>2</sub> fragment. <sup>e</sup> TME Ct corresponds to the centroid of the coordinating atoms of the TME ligand, and Cp\*Ct corresponds to the centroid of the central Cp.

lengths and angles that are in agreement with those found in ( $\eta^3$ : $\eta^3$ -C<sub>8</sub>H<sub>12</sub>)[Co(CO)<sub>3</sub>]<sub>2</sub> and ( $\eta^3$ -C<sub>3</sub>H<sub>5</sub>)Co(CO)<sub>3</sub>.<sup>35</sup>

The crystal structure of **2** (Figure 3) is very similar to that of **1**, showing the planarity of the hydrocarbon ligand and the central carbon atom (C<sub>Cent</sub>) barely displaced from the plane defined by the four terminal carbon atoms (0.048(2) Å). The cobalt atom is displaced by 1.7837(3) Å along the normal to the plane defined by its coordinated allyl carbon atoms. The carbonyl groups are in a staggered configuration relative to the PMe<sub>3</sub> group. **2** presents a similar asymmetry of the carbonyl groups to that of **1**. However, the Co–CO bond lengths are shorter due to the electron-donating influence from the PMe<sub>3</sub> group. There is also a general trend that distances between the metal and the atoms in the allyl-TME ligand are slightly longer in the compounds with a coordinated phosphine ligand. The Co–P bond lengths observed for **1–5** range between 2.1318(6)–2.1902(4) Å and compare closely to the value of 2.185(1) Å found in the related complex ( $\eta^3$ -C<sub>3</sub>H<sub>5</sub>)Co(CO)<sub>2</sub>PPh<sub>3</sub>.<sup>36</sup>

The bond angles found within the TME fragment for **2–6** are in agreement with those found in **1**, as expected considering the PMe<sub>3</sub> group mostly affects the metal center and the carbonyl ligands. The difference between the two Co–C(CO)–O(CO) carbonyl angles is increased for compounds **2–6**, mainly due to the  $\pi$ -bonding between the metal center and

the allyl fragment, which has an asymmetric effect on the carbonyl groups. The bond angle C(CO)–Co–C(CO) for **2** is slightly larger than the equivalent for **1** as a consequence of the staggered configuration, which allows an increased separation between the carbonyl groups. The two C(CO)–Co–P bond angles are reduced compared to the C(CO)–Co–C(CO) angles in **1** in order to minimize the interaction between the methyl groups of the PMe<sub>3</sub> fragment. It is possible to see the effect of the hydrogen atoms from the allyl fragment and from the PMe<sub>3</sub> group on the bond angles Co–P–C(PMe<sub>3</sub>): the Co1–P1–C8 angle is bigger than the other two (Figure 3).

In complexes **2–6**, we observe subtle variations in the distance between the Co and the terminal carbon atoms of the TME fragment which could be due to the increasing bulk of the phosphine substituents and the resulting proximity of the alkyl group to the allyl fragment. The size of the phosphine substituents has really little influence on the Co–P distance.

The crystal structure of 1<sup>+</sup>d (Figure 4) shows both Co(CO)<sub>x</sub> groups in a *syn*-configuration and not *anti* as in **1–6**. Only one [BF<sub>4</sub>]<sup>–</sup> group is present, suggesting that only one cobalt atom has been oxidized, with the loss of CO. The bond lengths between cobalt atoms and carbonyl carbon atoms are slightly longer than those found in **1** and more asymmetric (reflecting the differing oxidation states). The cobalt atoms are separated by 3.1079(5) Å, suggesting that there is no direct interaction between the metal centers since the Co–Co bond length reported for the related complexes of the type [Co<sub>2</sub>(CO)<sub>6</sub>L<sub>2</sub>] is 2.6 Å (L = CO, P(Oi-Pr)<sub>3</sub>, Pn-Bu<sub>3</sub>, PMe<sub>3</sub>).<sup>37</sup>

(34) In general, distances between planes cannot be given, because (except in special cases) the distance varies depending on where the distance is measured. However, because the hydrocarbon ligand is composed of two three-atom allyl fragments related by an inversion center, the two allyl planes are rigorously planar and rigorously parallel. The error on this distance is difficult to evaluate; however, the range of values for the six structures is 0.167–0.193 (mean = 0.184; standard deviation = 0.009). Thus, although the distance is small, the consistency and systematic nature of effect support the premise that this is significant.

(35) Cann, K.; Riley, P. E.; Davis, R. E.; Pettit, R. *Inorg. Chem.* **1978**, *17*, 1421.

(36) Rinze, P. V.; Mueller, U. *Chem. Ber.* **1979**, *112*, 1973.

(37) (a) Bryan, R. F.; Manning, A. R. *Chem. Commun. (Cambridge, U. K.)* **1968**, 1316. (b) Ibers, J. A. *J. Organomet. Chem.* **1968**, *14*, 423. (c) Jones, R. A.; Seeberger, M. H.; Stuart, A. L.; Whittlesey, B. R.; Wright, T. C. *Acta Crystallogr., Sect. C: Cryst. Struct. Commun.* **1986**, *42*, 399. (d) Farrar, D. H.; Lough, A. J.; Poe, A. J.; Stromnova, T. A. *Acta Crystallogr., Sect. C: Cryst. Struct. Commun.* **1995**, *51*, 2008.

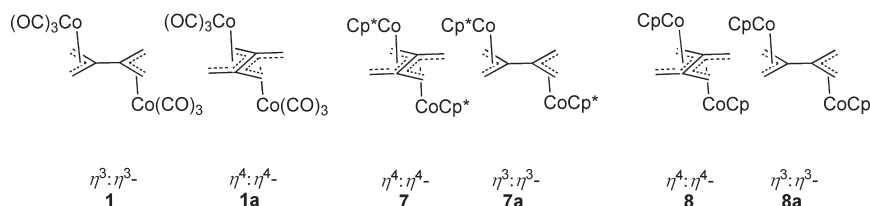


**Figure 7.** Possible isomers of TME[Co(CO)<sub>3</sub>]<sub>2</sub> (**1**, **1a**), TME[CoCp\*]<sub>2</sub> (**7**, **7a**), and TME[CoCp]<sub>2</sub> (**8**, **8a**).

**Table 6.** Selected Experimental and Calculated Bond Lengths (Å) for **1** and **7** and Calculated Bond Lengths for **8**

	<b>1</b>		<b>7</b>		<b>8</b>
	calculated	experimental <sup>a</sup>	calculated	experimental <sup>a</sup>	calculated
C <sub>Cent</sub> –C <sub>Term</sub>	1.41	1.414, 1.420	1.43	1.433, 1.453	1.43
C <sub>Cent</sub> –C <sub>Cent</sub> *	1.46	1.487	1.56	1.546	1.54
Co–C <sub>Term</sub>	2.07	2.080, 2.091	1.98	2.009, 2.011	1.99
Co–C <sub>Cent</sub>	2.01	2.017	1.99	2.011	2.00
Co–C <sub>Cent</sub> *	2.97	2.988	1.99	2.012	2.00

<sup>a</sup> Experimental values for **1** and **7** were obtained from the crystal structure data.

Analogous to **1**–**6**, complex **7** is located on a crystallographic center of inversion with approximate (noncrystallographic) *C*<sub>2h</sub> symmetry. The carbon atoms of the TME fragment are approximately coplanar, but careful examination of the difference map and refinement of the hydrogen atoms show that they are significantly out of plane. Despite the challenges classically associated with finding hydrogen atoms in the difference map, the data are generally good for all eight structures reported herein, and, though most obvious for **7**, the trend is visible in all cases (Figure 5). This deviation is probably due to increased  $\sigma$ -character in the Co–C bonds, leading to a distortion of the terminal carbon atoms toward tetrahedral geometry. Distortion of hydrogen atoms from the plane defining the  $\pi$ -bonded hydrocarbon has been seen previously.<sup>38</sup>

The cobalt atom lies 1.5432(2) Å along the normal to the plane defined by the four coordinated allyl carbon atoms, which is considerably shorter than the 1.7837(3) Å seen for **2**, reflecting the change from  $\eta^3$  to  $\eta^4$  binding. The Co–Cp\* Ct (Ct = centroid) distance is 1.6698(2) Å (Figure 6) and is in close agreement to 1.70 Å, which is the distance observed for Cp<sub>2</sub>Co<sup>39</sup> and Cp\*Co(acac).<sup>40</sup>

The bond lengths C<sub>Cent</sub>–C<sub>Term</sub> for **7** (1.434(3) and 1.453(2) Å) are slightly longer than those found for **1** (1.414(3) and 1.420(3) Å), but very similar to the C–C distances for the arene group in  $\mu$ - $\eta^4$ : $\eta^4$ -(C<sub>6</sub>H<sub>5</sub>*i*-Pr)[Cp\*Co]<sub>2</sub> (approximately 1.440 Å).<sup>24</sup> In fact, in **7** the cobalt atoms lie 1.5432(2) Å away from the best plane of the four coordinated allyl carbon atoms, whereas in **1**, they lie 1.7862(2) Å away from the best plane of the three coordinated allyl carbon atoms.

The coplanarity of the ligand forces the Cp\* ring to tilt in order to minimize the interaction between the hydrogen atoms from both fragments. The tilt angle is 10.7° (angle between the best planes of the TME fragment and the Cp\* ring) and forces the TME Ct–Co–Cp\* Ct bond angle to be less than 180°. This tilt is responsible for the approximately three differing bond lengths between Co1 and the carbon atoms of the Cp\* ring (2.098, ca. 2.068, and ca. 2.046 Å). The

longest bond length corresponds to Co1–C4, which lies above the allyl unit, due to steric hindrance caused by the TME ligand. In contrast, the bond lengths to C7 and C6 are the smallest, as they lie furthest from the TME ligand (Figure 6). Thermal ellipsoid plots of complexes **3**–**6** are given in the SI (Figures S1–S4).

**Structure and Bonding of TME Complexes.** In order to understand the ability of the TME ligand to adopt an  $\eta^3$ : $\eta^3$ - or  $\eta^4$ : $\eta^4$ -configuration depending on the nature of the bound transition metal fragment, a computational study was undertaken. The complexes considered were two coordination isomers for the Co(CO)<sub>3</sub> fragment, **1** and **1a**, and the two model isomers for the CoCp\* fragment, **8a** and **8**, where the Cp\* ring was replaced by Cp for computational expedience (Figure 7). Calculations were also carried out on the monocations **1**<sup>+</sup> and **8**<sup>+</sup> to study the electronic delocalization within these complexes. Fixing the symmetry as *C*<sub>2h</sub> enabled geometry optimization in both the  $\eta^3$ : $\eta^3$ - and  $\eta^4$ : $\eta^4$ -mode for both complexes.

By comparing the relative energies of the isomers, the two Co(CO)<sub>3</sub> fragments prefer the  $\eta^3$ : $\eta^3$ -configuration (**1**), whereas the two CoCp fragments prefer the  $\eta^4$ : $\eta^4$ -configuration (**8**). The two fragments Co(CO)<sub>3</sub> and CoCp are isolobal yet not isoelectronic, the former having an electron count of 15 and the latter 14. Thus the preference of Co(CO)<sub>3</sub> for  $\eta^3$ -coordination and CoCp for  $\eta^4$ -coordination is not unexpected and is in agreement with the 18-electron rule in both cases. The energy difference between **1** and **1a** is 136 kJ mol<sup>–1</sup> in favor of **1**. By contrast the isomer **8** is only 12 kJ mol<sup>–1</sup> favored compared to **8a**. The isomer **8a** was found to have a triplet ground state, indicating electron deficiency. Both **8** and **8a** were shown to be local minima by frequency calculations. Calculations were also carried out on **7** and **7a** (Figure 7). Isomer **7** was found to be favored by 18 kJ mol<sup>–1</sup>.

The calculated structures of the complexes are similar to those obtained experimentally for **1** and **7**. Both systems maintain a relatively planar C<sub>6</sub> skeleton, but in the case of **7**, the CH<sub>2</sub> groups are twisted to direct the  $\pi$ -orbitals toward the Co atoms. Table 6 compares the calculated and experimental bond lengths for the complexes **1**, **7**, and **8**. The calculations reproduce the experimentally determined dimensions well even when the methyl groups for the Cp\* ring were not considered in the computational model of **8**. In essence, **8** displays longer bond distances for the TME fragment C<sub>Cent</sub>–C<sub>Cent</sub>\*

(38) (a) Cooper, R. I.; Thompson, A. L.; Watkin, D. J. *J. Appl. Crystallogr.* **2010**, in press. (b) Rees, B.; Coppens, P. *Acta Crystallogr., Sect. B: Struct. Sci.* **1973**, *B* 29, 2516.

(39) Bunder, W.; Weiss, E. *J. Organomet. Chem.* **1975**, *92*, 65.

(40) Smith, M. E.; Andersen, R. A. *J. Am. Chem. Soc.* **1996**, *118*, 11119.

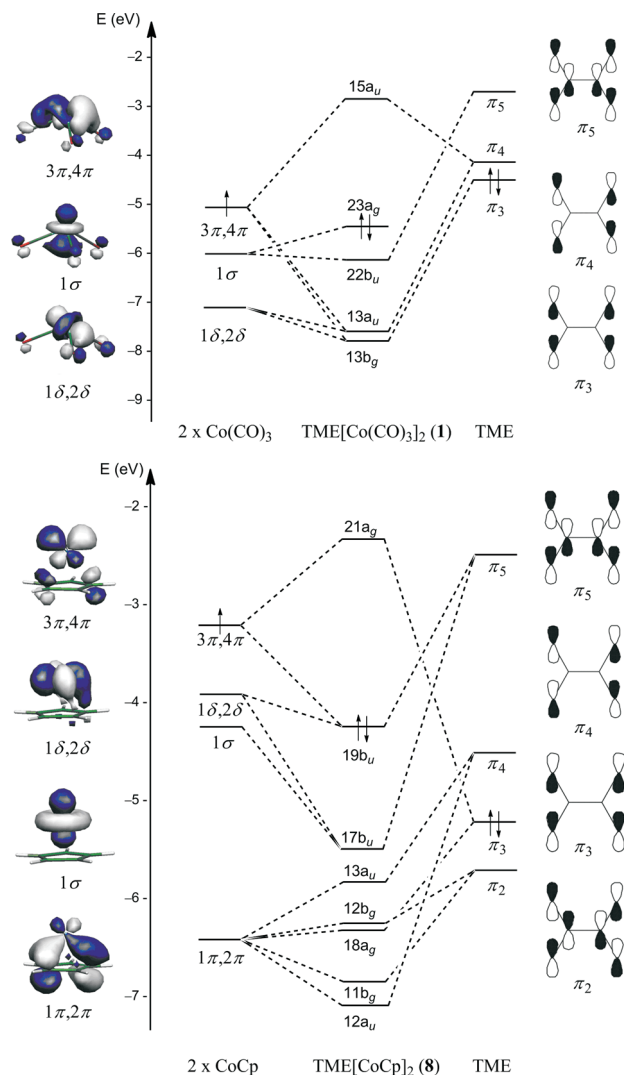


**Figure 8.** Molecular orbital interaction schemes for **1** and **8**. (The  $2\sigma$  orbital lies at higher energy.)

whereas **1** presents longer  $\text{Co}-\text{C}_{\text{Term}}$  and  $\text{Co}-\text{C}_{\text{Cent}}$  distances. The optimized structures of **1** and **8** are depicted in the SI (Figure S5).

The bonding in complexes **1** and **8** can be described by considering the interaction of two  $\text{Co}(\text{CO})_3$  and two  $\text{CoCp}^*$  fragments ( $\text{Co}_{\text{frag}}$ ), respectively, with the TME ligand. The fragments retain their individual geometries in the whole molecule and are in a singlet spin state due to restricted point calculations. The orbitals of the molecule are then described as linear combinations of fragment orbitals (FOs). Both fragments give three frontier orbitals ( $2\sigma$ ,  $3\pi$ , and  $4\pi$ ) for binding to the TME ligand.

For  $\text{Co}(\text{CO})_3$ , six d-electrons on each Co center are held in a “ $t_{2g}$ ” set of orbitals; they are labeled  $1\sigma$ ,  $1\delta$ , and  $2\delta$ , indicating their symmetry with respect to the rotational axis of the  $\text{Co}(\text{CO})_3$  fragment. These three orbitals back-bond to the CO groups. A similar effect is seen in the complex  $\text{TME}[\text{Fe}(\text{CO})_3]_2$ , where the fragment  $\text{Fe}(\text{CO})_3$  presents three lower energy metal-type orbitals (six d-electrons), which are heavily involved in  $\text{Fe}-\text{CO}$  back-bonding and hardly interact with the TME fragment.<sup>41</sup> For  $\text{CoCp}$ , the electrons in the

“ $t_{2g}$ ” set of orbitals (again denoted  $1\sigma$ ,  $1\delta$ , and  $2\delta$ ) of the  $\text{CoCp}$  fragment differ in that they are virtually nonbonding.

The orbital interaction schemes for **1** and **8** are depicted in Figure 8. The  $\text{Co}_{\text{frag}}$  FOs are labeled according to the fragment axis rotational symmetry. The resultant MOs are labeled according to their  $C_{2h}$  symmetry. The relevant FOs of the  $\text{Co}(\text{CO})_3$ ,  $\text{CoCp}$ , and TME fragments are illustrated in the diagram. The isosurfaces of selected MOs of **1** and **8** are depicted in the SI (Figures S6 and S7).

The  $\text{CoCp}$  FOs are significantly higher in energy than the corresponding FOs of  $\text{Co}(\text{CO})_3$ . This leads to greater mixing with the TME  $\pi$ -orbitals and more back-bonding from the metal to the TME ligand in **8** than **1**. The degree of occupancy of the various FOs in the complex is shown in Table 7. For **1** the  $1\sigma$ ,  $1\pi$ , and  $2\pi$  FOs effectively retain their full complement of two electrons, indicating that back-bonding to the CO ligands is not perturbed on complexation. For **8** the FOs  $1\sigma$ ,  $1\pi$ , and  $2\pi$  lose electrons by back-bonding to the TME ligand. The occupancies of the TME fragment  $\pi$ -orbitals demonstrate that both donation to the metal from TME and acceptance of electrons into the unoccupied  $\pi$ -orbitals ( $\pi_4$  to  $\pi_6$ ) are greater on interaction with  $\text{CoCp}$  to form **8** than  $\text{Co}(\text{CO})_3$  to give **1**; thus the  $\text{Co}-\text{C}$  bond lengths are shorter in **8** than **1**. Also the net result is a greater negative charge on TME in **8** than **1** (Table 7). The direct consequence of this increased charge is the lengthening of the bonds in the TME fragment.

**Delocalization in Monocations  $1^+$  and  $8^+$ .** In order to analyze whether or not the two metal centers are isolated from each other, spin polarization calculations were performed. In both cases, the unpaired electron was attributed to one metal center, and the structure was optimized. Both complexes were optimized in a doublet spin state. For complexes  $1^+$  and  $8^+$ , the spin density relaxed during the optimization so that, in the optimized structure, the spin density on both Co centers was approximately equal (0.42 and 0.38 electron on each Co atom in  $1^+$  and  $8^+$ , respectively). The results indicate that the removal of one electron on each complex leads to the corresponding cation in which the spin density is delocalized on both metal centers, consistent with the electrochemical data.

## Conclusion

We have synthesized a series of dicobalt complexes containing the TME ligand. Structural and spectroscopic data indicate the coplanarity of the TME ligand and its ability to adopt different coordination modes ( $\eta^3:\eta^3$  or  $\eta^4:\eta^4$ ) according to the electron number of the Co centers and the ancillary ligands. Electrochemical studies suggested electronic communication of Co centers through the ligand in all complexes studied. DFT calculations show the  $\eta^3:\eta^3$ -binding mode to be significantly more stable for  $\text{TME}[\text{Co}(\text{CO})_3]_2$  than  $\eta^4:\eta^4$ -coordination. For  $\text{TME}[\text{CoCp}^*]_2$  the  $\eta^4:\eta^4$ -mode is energetically favored over  $\eta^3:\eta^3$  by a lesser amount, but the  $\eta^3:\eta^3$ -complex is predicted to be a biradical. TME binds  $\text{CoCp}^*$  more strongly than  $\text{Co}(\text{CO})_3$  and carries a larger negative charge, with two  $\text{CoCp}^*$  ligands accounting for the longer  $\text{C}-\text{C}$  and shorter  $\text{Co}-\text{C}$  bonds in this complex.

## Experimental Details

All reactions were carried out under an inert atmosphere of nitrogen using standard Schlenk line techniques<sup>42</sup> or a Braun

(41) Thorn, D. *Inorg. Chem.* **1978**, *17*, 126.

(42) Errington, R. J. *Advanced Practical Inorganic and Metalorganic Chemistry*; Blackie A+P: London, 1997.

**Table 7. Occupancy of FOs in 1 and 8 and Charges on the Fragments TME and Co<sub>frag</sub>**

	TME							Co <sub>frag</sub>						
	$\pi_1$	$\pi_2$	$\pi_3$	$\pi_4$	$\pi_5$	$\pi_6$	charge	$1\sigma$	$1\delta$	$2\delta$	$3\pi$	$4\pi$	$2\sigma$	charge
<b>1</b>	1.79	1.67	0.97	0.92	0.42	0.10	-0.11	1.98	1.98	1.96	1.74	1.08	0.34	+0.06
<b>8</b>	1.70	1.44	1.26	1.09	0.71	0.19	-0.64	1.97	1.84	1.91	1.03	0.82	0.4	+0.32

Unilab glovebox, unless stated otherwise. Where necessary, solvents were dried by reflux over an appropriate drying agent [sodium-benzophenone diketyl (THF), sodium (toluene), sodium-potassium alloy (Et<sub>2</sub>O, pentane), calcium hydride (CH<sub>2</sub>Cl<sub>2</sub>, MeCN)] or by passage through a column of activated alumina (hexane). Deuterated solvents for NMR spectroscopy of air-sensitive materials were dried by reflux over the appropriate drying agent and purified by trap-to-trap distillation: potassium (C<sub>6</sub>D<sub>6</sub>, toluene-*d*<sub>8</sub>).

NMR spectra were recorded using a Varian Mercury VX-Works 300 MHz spectrometer or a Varian Venus 300 MHz spectrometer. <sup>1</sup>H and <sup>13</sup>C spectra were referenced to the residual protio-solvent peak; <sup>31</sup>P spectra were referenced externally to H<sub>3</sub>PO<sub>4</sub>. Oxygen- or water-sensitive samples were prepared using dried solvents under an inert atmosphere in a glovebox. They were then sealed in tubes fitted with Young's-type concentric stopcocks. Fourier transform infrared spectra were recorded on a Perkin-Elmer Paragon 1000 FT-IR spectrometer (range used 4000–400 cm<sup>-1</sup>, resolution 1 cm<sup>-1</sup>) as KBr discs. In the case of air-sensitive complexes, samples were ground with KBr powder and loaded into a die in a glovebox, before being quickly pressed into a disk on the open bench. The spectrum was run immediately to prevent decomposition. Elemental analyses for air-sensitive complexes were performed by the Elemental Analysis Service, London Metropolitan University, London, and mass spectra by the Mass Spectrometry Service, Chemistry Research Laboratory, University of Oxford. Electrochemical measurements were performed using an EG&G Princeton Applied Research model 273 potentiostat/galvanostat and a CH Instruments electrochemical analyzer (the potentiostat was controlled by a PC running CH Instruments version 2.05 electrochemical software), at room temperature. All measurements were made using a standard three-electrode setup: a platinum disk working electrode, a platinum mesh counter electrode, and a AgCl/Ag reference electrode. The cell was specially constructed for air-sensitive samples, having a side arm fitted with a Young's tap. Cyclic voltammetry measurements were made under an atmosphere of nitrogen on deoxygenated solutions of ca. 10<sup>-3</sup> M with 0.1 M [*n*-Bu<sub>4</sub>N]<sup>+</sup>[BF<sub>4</sub>]<sup>-</sup> as supporting electrolyte added and using an appropriate dry solvent. Redox potentials were referenced to the [Cp<sub>2</sub>Fe]<sup>+/0</sup>/Cp<sub>2</sub>Fe couple at 0 mV. The reversibility of the redox couple was judged by comparison with the behavior of the [Cp<sub>2</sub>Fe]<sup>+/0</sup>/Cp<sub>2</sub>Fe couple under identical conditions (506 mV in THF, 406 mV in CH<sub>2</sub>Cl<sub>2</sub>, and 400 mV in MeCN, relative to SCE).<sup>43</sup>

Single-crystal X-ray diffraction experiments were carried out on crystals that were mounted on a glass fiber or hair using perfluoropolyether oil and quench cooled to 150 K in a stream of cold liquid nitrogen using an Oxford Cryosystems CryoStream unit.<sup>44</sup> Data collection was performed using an Enraf-Nonius FR590 KappaCCD diffractometer using graphite-monochromated Mo K $\alpha$  X-ray radiation ( $\lambda = 0.71073$  Å). Intensity data were

processed (including interframe scaling and unit cell refinement) using Denzo-SMN/Scalepack.<sup>45</sup> The structures were then solved using direct methods with either SIR92<sup>46</sup> (compounds **1**, **1**<sup>+</sup>**d**, **3**, and **7**) or ShelXS<sup>47</sup> (compounds **2** and **4–6**). Subsequent full-matrix least-squares refinement was carried out using either the CRYSTALS program suite<sup>48</sup> (compounds **1**, **1**<sup>+</sup>**d**, **3**, and **7**) or ShelXL<sup>47</sup> (compounds **2** and **4–6**). All structures have been deposited with the Cambridge Crystallographic Data Center, CCDC. Copies of these data can be obtained free of charge from The Cambridge Crystallographic Data Center via www.ccdc.cam.ac.uk/data\_request/cif.

DFT calculations were carried out using the Amsterdam Density Functional program (ADF) versions 2004.01 and 2009.01.<sup>49</sup> Scalar relativistic corrections were included via the zero-order regular approximation (ZORA) method,<sup>50</sup> together with the nonlocal exchange correction by Becke<sup>51</sup> and nonlocal correlation corrections by Perdew.<sup>52</sup> Geometry optimizations were performed at the LDA level and exchange and correlation corrections applied post-SCF. The Slater-type orbital basis sets were of triple- $\zeta$  quality augmented with a single polarization function and two diffuse functions (ADF basis TZP). The core electrons of Co atoms were frozen up to 3p. Optimizations were performed without symmetry restraints. Fragment calculations were performed to enable analysis of the orbital interactions of the Co(CO)<sub>3</sub> and CpCo fragments, respectively, with the TME fragment. In these calculations the complex is divided into two fragments, whose molecular and electronic structures are calculated in a single-point optimization with a restricted singlet spin state. The geometry of the fragment is preserved from the optimized structure of the full complex. The molecular orbitals (MOs) of the complex are formed through a linear combination of the MOs of the two fragments.

All reagents were used as received, unless specified otherwise. PEt<sub>3</sub>, P*n*-Bu<sub>3</sub>, PPh<sub>3</sub>, and P(OPh)<sub>3</sub> were distilled prior to use (very toxic). AgBF<sub>4</sub> and NaPF<sub>6</sub> were supplied by Sigma-Aldrich, United Kingdom. The following compounds were prepared according to published procedures: TMEBr<sub>2</sub>,<sup>53</sup> Na[Co(CO)<sub>4</sub>],<sup>54</sup> KO*t*-Am,<sup>55</sup> Cp\*Li.<sup>56</sup>

**Preparation of ( $\eta^3$ : $\eta^3$ -TME)[Co(CO)<sub>3</sub>]<sub>2</sub>, **1**.** TMEBr<sub>2</sub> (10.0 g, 4.17 mmol) was dissolved in hexane (100 mL) and filtered through dried MgSO<sub>4</sub>, then added to a solution of Na[Co(CO)<sub>4</sub>]

(47) Sheldrick, G. M. *Acta Crystallogr. A* **2008**, *64*, 112.

(48) Betteridge, P. W.; Carruthers, J. R.; Cooper, R. I.; Prout, K.; Watkin, D. J. *J. Appl. Crystallogr.* **2003**, *36* (pt.6), 1487.

(49) (a) Te Velde, G.; Bickelhaupt, F. M.; Baerends, E. J.; Fonseca Guerra, C.; van Gisbergen, S. J. A.; Snijders, J. G.; Ziegler, T. *J. Comput. Chem.* **2001**, *22*, 931. (b) Fonseca Guerra, C.; Snijders, J. G.; te Velde, G.; Baerends, E. J. *Theor. Chem. Acc.: Theor., Comput., Model. (Theor. Chim. Acta)* **1998**, *99*, 391.

(50) (a) van Lenthe, E.; Baerends, E. J.; Snijders, J. G. *J. Chem. Phys.* **1993**, *99*, 4597. (b) van Lenthe, E.; Baerends, E. J.; Snijders, J. G. *J. Chem. Phys.* **1994**, *101*, 9783. (c) van Lenthe, E.; Ehlers, A.; Baerends, E. J. *J. Chem. Phys.* **1999**, *110*, 8943. (d) van Lenthe, E.; Snijders, J. G.; Baerends, E. J. *J. Chem. Phys.* **1996**, *105*, 6505. (e) van Lenthe, E.; van Leeuwen, R.; Baerends, E. J.; Snijders, J. G. *Int. J. Quantum Chem.* **1996**, *57*, 281.

(51) (a) Becke, A. D. *Phys. Rev. A* **1988**, *38*, 3098. (b) Becke, A. D. *J. Chem. Phys.* **1988**, *88*, 1053.

(52) Perdew, J. P.; Yue, W. *Phys. Rev. B* **1986**, *33*, 8800.

(53) Gaoni, Y.; Sadeh, S. *J. Org. Chem.* **1980**, *45*, 870.

(54) Edgell, W. F.; Lyford, J. *Inorg. Chem.* **1970**, *9*, 1932.

(55) Lochmann, L.; Trekoval, J. *J. Organomet. Chem.* **1987**, *326*, 1.

(56) (a) Feitler, D.; Whitesides, G. M. *Inorg. Chem.* **1976**, *15*, 466.

(b) Fendrick, C. M.; Schertz, L. D.; Mintz, E. A.; Marks, T. J. *Inorg. Synth.* **1992**, *29*, 193.

(43) (a) Barlow, S. *Inorg. Chem.* **2001**, *40*, 7047. (b) Connelly, N. G.; Geiger, W. E. *Chem. Rev. (Washington, DC, U. S.)* **1996**, *96*, 877.

(44) Cosier, J.; Glazer, A. M. *J. Appl. Crystallogr.* **1986**, *19*, 105.

(45) Otwinowski, Z.; Minor, W. *Methods in Enzymology: Macromolecular Crystallography, Part A*; Academic Press: San Diego, CA, 1997; Vol. 276, p 307.

(46) Altomare, A.; Cascarano, G.; Giacovazzo, C.; Guagliardi, A.; Burla, M. C.; Polidori, G.; Camalli, M. *J. Appl. Crystallogr.* **1994**, *27*, 435.

(1.620 g, 8.330 mmol) in THF (50 mL) at  $-80\text{ }^{\circ}\text{C}$ . The mixture was warmed to room temperature, and a white precipitate formed gradually. The solution was stirred for 15 h and the solvent removed under vacuum. The resulting lime green solid was extracted with toluene ( $3 \times 50\text{ mL}$ ) and filtered through Celite. This solution was reduced to minimum volume and stored at  $-80\text{ }^{\circ}\text{C}$  overnight. The yellow-orange solid formed was collected and dried under vacuum. Yield: 0.964 g (63.2%) (2.634 mmol).  $^1\text{H NMR}$  ( $\text{C}_6\text{D}_6$ )  $\delta$  (ppm): 1.36 (s, 4H,  $\text{C}_6\text{H}_8$ ), 2.85 (s, 4H,  $\text{C}_6\text{H}_8$ ).  $^{13}\text{C NMR}$  ( $\text{C}_6\text{D}_6$ )  $\delta$  (ppm): 45.10 (s, allyl terminal carbon), 98.21 (s, allyl central carbon), 202.75 (s, CO). IR (KBr)  $\text{cm}^{-1}$ : 1985, 2053. Anal. Calcd for  $\text{C}_{12}\text{H}_8\text{Co}_2\text{O}_6$ : C, 39.37; H, 2.20; Co, 32.97. Found: C, 40.05; H, 1.50; Co, 31.94. MS (EI)  $m/z$ : 365.898 ( $\text{M}^+$ ), 337.920 ( $\text{M}^+ - (\text{CO})$ ), 309.883 ( $\text{M}^+ - (\text{CO})_2$ ), 281.889 ( $\text{M}^+ - (\text{CO})_3$ ), 253.896 ( $\text{M}^+ - (\text{CO})_4$ ), 225.907 ( $\text{M}^+ - (\text{CO})_5$ ), 197.9048 ( $\text{M}^+ - (\text{CO})_6$ ). CV ( $\text{CH}_2\text{Cl}_2$ ) V:  $E_1 = +0.25$ ,  $E_2 = +0.50$  (both quasi-reversible).

**Preparation of  $\{\text{TME}[\text{Co}(\text{CO})_3\text{I}_2\text{P}(\text{O})\text{Ph}_3]_2\}^{2+}[\text{BF}_4]^{-}_2$ , **1**.** A solution of **1** (0.100 g, 0.274 mmol) in  $\text{CH}_2\text{Cl}_2$  (30 mL) was added to a solution of  $\text{AgBF}_4$  (0.106 g, 0.550 mmol) in  $\text{CH}_2\text{Cl}_2$  (30 mL). During the addition a dark solid precipitated and the solution turned dark green. After stirring for 15 min, all volatiles were removed under vacuum, leaving a dark green residue. This solid was washed with hexane ( $2 \times 15\text{ mL}$ ), then dissolved in  $\text{MeNO}_2$ , and the new solution was filtered into a new Schlenk. The  $\text{MeNO}_2$  solution was reduced to minimum volume and the solid precipitated by the dropwise addition of  $\text{Et}_2\text{O}$ . The precipitate was collected, washed with  $\text{Et}_2\text{O}$  (10 mL), and dried under vacuum to yield an orange solid. Yield: 0.015 g (10.3%) (0.028 mmol). Anal. Calcd for  $\text{C}_{12}\text{H}_8\text{Co}_2\text{O}_6\text{B}_2\text{F}_8$ : C, 26.71; H, 1.49. Found: C, 26.78; H, 1.50.

**Preparation of  $(\eta^3\text{-}\eta^3\text{-TME})[\text{Co}(\text{CO})_2\text{PMe}_3]_2$ , **2**.** A solution of **1** (0.050 g, 0.137 mmol) in THF (30 mL) was added to a solution of  $\text{PMe}_3$  (0.031 g, 0.41 mmol) in THF (30 mL). A slight gas evolution was observed with the mixture changing to a darker orange color. After stirring for 15 min, all volatiles were removed under vacuum, leaving a yellow solid. The solid was extracted with hexane ( $2 \times 15\text{ mL}$ ), and the solution was reduced to a minimum volume and stored at  $-35\text{ }^{\circ}\text{C}$  overnight. The orange crystalline solid formed was collected, washed at  $-35\text{ }^{\circ}\text{C}$  with hexane, and dried under vacuum. Yield: 0.028 g (43.6%) (0.060 mmol).  $^1\text{H NMR}$  ( $\text{C}_6\text{D}_6$ )  $\delta$  (ppm): 0.98 (d,  $J = 8.8\text{ Hz}$ , 18H,  $\text{PMe}_3$ ), 1.54 (s, 4H,  $\text{C}_6\text{H}_8$ ), 2.79 (d,  $J = 5.28\text{ Hz}$ , 4H,  $\text{C}_6\text{H}_8$ ).  $^{13}\text{C NMR}$  ( $\text{C}_6\text{D}_6$ )  $\delta$  (ppm): 20.12 (d,  $J = 27.64\text{ Hz}$ ,  $\text{PMe}_3$ ), 39.35 (d,  $J = 2.59\text{ Hz}$ , allyl terminal carbon), 98.14 (s, allyl central carbon), 205.01 (s, CO).  $^{31}\text{P NMR}$  ( $\text{C}_6\text{D}_6$ )  $\delta$  (ppm): 15.10 (s,  $\text{PMe}_3$ ). IR (KBr)  $\text{cm}^{-1}$ : 1917, 1968. Anal. Calcd for  $\text{C}_{16}\text{H}_{26}\text{O}_4\text{P}_2\text{Co}_2$ : C, 41.56; H, 5.67. Found: C, 41.73; H, 5.68. MS (EI)  $m/z$ : 461.995 ( $\text{M}^+$ ), 434.01 ( $\text{M}^+ - (\text{CO})$ ), 406.024. CV ( $\text{CH}_2\text{Cl}_2$ ) V:  $E_1 = -0.07$ ,  $E_2 = +0.15$  (both quasi-reversible).

**Preparation of  $(\eta^3\text{-}\eta^3\text{-TME})[\text{Co}(\text{CO})_2\text{PEt}_3]_2$ , **3**.** The same procedure for the synthesis of **2** was followed using **1** (0.050 g, 0.137 mmol) in THF (40 mL) and  $\text{PEt}_3$  (0.048 g, 0.410 mmol) in THF (40 mL). Yield: 0.025 g (31.4%) (0.043 mmol).  $^1\text{H NMR}$  ( $\text{C}_6\text{D}_6$ )  $\delta$  (ppm): 0.84 (m, 18H,  $\text{PCH}_2\text{CH}_3$ ), 1.24–1.38 (m, 12H,  $\text{PCH}_2\text{CH}_3$ ), 1.58 (s, 4H,  $\text{C}_6\text{H}_8$ ), 2.83 (d,  $J = 4.40\text{ Hz}$ , 4H,  $\text{C}_6\text{H}_8$ ).  $^{13}\text{C NMR}$  ( $\text{C}_6\text{D}_6$ )  $\delta$  (ppm): 8.39 (s,  $\text{PCH}_2\text{CH}_3$ ), 21.73 (d,  $J = 24.76\text{ Hz}$ ,  $\text{PCH}_2\text{CH}_3$ ), 38.81 (d,  $J = 2.30\text{ Hz}$ ,  $\text{C}_6\text{H}_8$ ), 98.33 (s,  $\text{C}_6\text{H}_8$ ), 205.90 (s, CO).  $^{31}\text{P NMR}$  ( $\text{C}_6\text{D}_6$ )  $\delta$  (ppm): 50.28 (s,  $\text{PEt}_3$ ). IR (KBr)  $\text{cm}^{-1}$ : 1920, 1957. Anal. Calcd for  $\text{C}_{22}\text{H}_{38}\text{O}_4\text{P}_2\text{Co}_2$ : C, 48.36; H, 7.01. Found: C, 48.54; H, 7.12. MS (EI)  $m/z$ : 118.076 ( $\text{PEt}_3$ ). CV ( $\text{CH}_2\text{Cl}_2$ ) V:  $E_1 = -0.27$ ,  $E_2 = +0.03$  (both quasi-reversible).

**Preparation of  $(\eta^3\text{-}\eta^3\text{-TME})[\text{Co}(\text{CO})_2\text{Pn-Bu}_3]_2$ , **4**.** The same procedure for the synthesis of **2** was followed using **1** (0.050 g, 0.137 mmol) in THF (40 mL) and  $\text{Pn-Bu}_3$  (0.083 g, 0.410 mmol) in THF (40 mL). Yield: 0.067 g (69.3%) (0.095 mmol).  $^1\text{H NMR}$  ( $\text{C}_6\text{D}_6$ )  $\delta$  (ppm): 0.86 (t,  $J = 7.34\text{ Hz}$ , 18H,  $\text{PCH}_2\text{CH}_2\text{CH}_2\text{-CH}_3$ ), 1.11–1.37 (m, 12H,  $\text{PCH}_2\text{CH}_2\text{CH}_2\text{CH}_3$ ), 1.38–1.50 (m, 12H,  $\text{PCH}_2\text{CH}_2\text{CH}_2\text{CH}_3$ ), 1.50–1.62 (m, 12H,  $\text{PCH}_2\text{CH}_2\text{-}$

$\text{CH}_2\text{CH}_3$ ), 1.74 (s, 4H,  $\text{C}_6\text{H}_8$ ), 3.02 (d,  $J = 4.11\text{ Hz}$ , 4H,  $\text{C}_6\text{H}_8$ ).  $^{13}\text{C NMR}$  ( $\text{C}_6\text{D}_6$ )  $\delta$  (ppm): 14.32 (s,  $\text{PCH}_2\text{CH}_2\text{CH}_2\text{CH}_3$ ), 25.17 (s,  $\text{PCH}_2\text{CH}_2\text{CH}_2\text{CH}_3$ ), 29.46 (s,  $\text{PCH}_2\text{CH}_2\text{CH}_2\text{CH}_3$ ), 29.78 (s,  $\text{PCH}_2\text{CH}_2\text{CH}_2\text{CH}_3$ ), 39.02 (d,  $J = 2.02\text{ Hz}$ , allyl terminal carbon), 98.84 (d,  $J = 0.86\text{ Hz}$ , allyl central carbon), 206.13 (s, CO).  $^{31}\text{P NMR}$  ( $\text{C}_6\text{D}_6$ )  $\delta$  (ppm): 42.17 (s,  $\text{Pn-Bu}_3$ ). IR (KBr)  $\text{cm}^{-1}$ : 1912, 1972. Anal. Calcd for  $\text{C}_{34}\text{H}_{62}\text{O}_4\text{P}_2\text{Co}_2$ : C, 57.12; H, 8.74; P, 8.67; Co, 16.50. Found: C, 57.24; H, 8.74; P, 8.76; Co, 16.30. MS (EI)  $m/z$ : 202.183 ( $\text{Pn-Bu}_3$ ). CV ( $\text{CH}_2\text{Cl}_2$ ) V:  $E_1 = -0.21$ ,  $E_2 = +0.07$  (both quasi-reversible).

**Preparation of  $(\eta^3\text{-}\eta^3\text{-TME})[\text{Co}(\text{CO})_2\text{PPh}_3]_2$ , **5**.** A solution of **1** (0.050 g, 0.137 mmol) in THF (40 mL) was added to a solution of  $\text{PPh}_3$  (0.108 g, 0.410 mmol) in THF (40 mL). After stirring for 15 min, all volatiles were removed under vacuum, leaving a yellow-orange, oily product. The residue was washed with hexane ( $2 \times 30\text{ mL}$ ) to remove unreacted  $\text{PPh}_3$ . The yellow solid was dissolved in the minimum volume of THF and layered with hexane. The crystalline solid obtained was collected, washed with hexane, and dried under vacuum. Yield: 0.050 g (43.8%) (0.060 mmol).  $^1\text{H NMR}$  ( $\text{C}_6\text{D}_6$ )  $\delta$  (ppm): 1.44 (d,  $J = 4.40\text{ Hz}$ , 4H,  $\text{C}_6\text{H}_8$ ), 2.89 (d,  $J = 3.52\text{ Hz}$ , 4H,  $\text{C}_6\text{H}_8$ ), 6.87–7.06 (m, two superimposed peaks, 18H,  $\text{PPh}_3$ ), 7.44–7.67 (m, 12H,  $\text{PPh}_3$ ).  $^{13}\text{C NMR}$  ( $\text{C}_6\text{D}_6$ )  $\delta$  (ppm): 43.28 (s, allyl terminal carbon), 99.15 (s, allyl central carbon), 128.75, 128.88, 133.85, 134.00, 136.54, and 137.05 (all s,  $\text{PPh}_3$ ), 130.06 (d,  $J = 2.30\text{ Hz}$ ,  $\text{PPh}_3$ ), 206.13 (s, CO).  $^{31}\text{P NMR}$  ( $\text{C}_6\text{D}_6$ )  $\delta$  (ppm): 58.82 (s,  $\text{PPh}_3$ ). IR (KBr)  $\text{cm}^{-1}$ : 1918, 1974. Anal. Calcd for  $\text{C}_{46}\text{H}_{38}\text{O}_4\text{P}_2\text{Co}_2$ : C, 66.19; H, 4.58; P, 7.42; Co, 14.12. Found: C, 66.26; H, 4.59; P, 7.34; Co, 14.09. MS (EI)  $m/z$ : 262.071 ( $\text{PPh}_3$ ). CV ( $\text{CH}_2\text{Cl}_2$ ) V:  $E_1 = -0.03$  (quasi-reversible),  $E_2 = +0.39$  (irreversible oxidation).

**Preparation of  $(\eta^3\text{-}\eta^3\text{-TME})[\text{Co}(\text{CO})_2\text{P}(\text{O}^i\text{Pr})_3]_2$ , **6**.** A solution of **1** (0.100 g, 0.273 mmol) in THF (50 mL) was added to a solution of  $\text{P}(\text{O}^i\text{Pr})_3$  (0.169 g, 0.547 mmol) in THF (50 mL). After stirring for 15 min, the solution was concentrated to 20 mL and layered with hexane. The crystalline solid formed was collected, washed with hexane, and dried under vacuum. Yield: 0.162 g (63.8%) (0.174 mmol).  $^1\text{H NMR}$  ( $\text{C}_6\text{D}_6$ )  $\delta$  (ppm): 1.63 (d,  $J = 12.21\text{ Hz}$ , 4H,  $\text{C}_6\text{H}_8$ ), 3.16 (d,  $J = 1.76\text{ Hz}$ , 4H,  $\text{C}_6\text{H}_8$ ), 6.81–6.93 (m, 6H,  $\text{P}(\text{O}^i\text{Pr})_3$ ), 6.96–7.11 (m, 12H,  $\text{P}(\text{O}^i\text{Pr})_3$ ), 7.24 (m, 12H,  $\text{P}(\text{O}^i\text{Pr})_3$ ).  $^{13}\text{C NMR}$  ( $\text{C}_6\text{D}_6$ )  $\delta$  (ppm): 43.66 (s, allyl terminal carbon), 97.75 (s, allyl central carbon), 122.20 (d,  $J = 4.61\text{ Hz}$ ,  $\text{P}(\text{O}^i\text{Pr})_3$ ), 125.34 (s,  $\text{P}(\text{O}^i\text{Pr})_3$ ), 130.30 (s,  $\text{P}(\text{O}^i\text{Pr})_3$ ), 152.47 (d,  $J = 6.05\text{ Hz}$ , C bound to the O atom in  $\text{P}(\text{O}^i\text{Pr})_3$ ), 205.05 (s, CO).  $^{31}\text{P NMR}$  ( $\text{C}_6\text{D}_6$ )  $\delta$  (ppm): 160.51 (s,  $\text{P}(\text{O}^i\text{Pr})_3$ ). IR (KBr)  $\text{cm}^{-1}$ : 1962, 1969, 2009. Anal. Calcd for  $\text{C}_{46}\text{H}_{38}\text{O}_{10}\text{P}_2\text{Co}_2$ : C, 59.35; H, 4.11. Found: C, 59.12; H, 6.03 (slightly impure probably due to decomposition). MS (EI)  $m/z$ : No relevant signals were observed. CV ( $\text{CH}_2\text{Cl}_2$ ) V:  $E_1 = -0.05$  (quasi-reversible),  $E_2 = +0.36$  (irreversible oxidation).

**Preparation of TMEK<sub>2</sub>.** The synthesis was adapted from the literature preparation of TMEK<sub>2</sub>.<sup>57</sup> A solution of  $n\text{-BuLi}$  (60 mL, 0.150 mol) in hexane (25 mL) was carefully added to a suspension of  $\text{KO}^t\text{-Am}$  (18.240 g, 0.145 mol) in hexane (40 mL). The mixture was cooled to  $-80\text{ }^{\circ}\text{C}$ , and a solution of 2,3-dimethyl-1,3-butadiene (9.18 mL, 0.081 mol) in hexane (30 mL) was added dropwise. After stirring for 1 h at room temperature, the orange solid was collected, washed with hexane ( $3 \times 50\text{ mL}$ ), and dried thoroughly under vacuum. The pyrophoric yellow powder obtained was used without further purification. Yield: 11.520 g (90.1%) (0.073 mol).

**Preparation of  $(\eta^4\text{-}\eta^4\text{-TME})[\text{CoCp}^*]_2$ , **7**.** A suspension of  $\text{Cp}^*\text{Li}$  (1.775 g, 0.013 mmol) in THF was cooled to  $-80\text{ }^{\circ}\text{C}$ , and a solution of  $\text{Co}(\text{acac})_2$  (3.190 g, 0.013 mmol) in THF (40 mL) was added dropwise. After stirring for 4.5 h at room temperature, the mixture was cooled to  $-80\text{ }^{\circ}\text{C}$  and a suspension of TMEK<sub>2</sub> (1 g, 0.006 mmol) in THF (40 mL) was slowly added. After stirring for 12 h at room temperature, all volatiles were removed under vacuum. The residue was extracted with pentane

(3 × 50 mL). This resulting solution was filtered through Celite, reduced to minimum volume, and stored at -80 °C overnight. The dark purple microcrystalline solid obtained was collected and dried under vacuum. Yield: 1.100 g (37.9%) (0.002 mmol). <sup>1</sup>H NMR (C<sub>6</sub>D<sub>6</sub>) δ (ppm): -0.44 (d, *J* = 2.00 Hz, 4H, C<sub>6</sub>H<sub>8</sub>), 1.71 (s, 30H, Cp\*), 1.77 (d, *J* = 2.00 Hz, 4H, C<sub>6</sub>H<sub>8</sub>). <sup>13</sup>C NMR (C<sub>6</sub>D<sub>6</sub>) δ (ppm): 10.15 (s, C<sub>5</sub>Me<sub>5</sub>), 26.87 (s, allyl terminal carbon), 69.67 (s, allyl central carbon), 89.18 (s, C<sub>5</sub>Me<sub>5</sub>). Anal. Calcd for C<sub>26</sub>H<sub>38</sub>Co<sub>2</sub>: C, 66.66; H, 8.18. Found: C, 66.74; H, 8.22. MS

(EI) *m/z*: 468.165 (M<sup>+</sup>), 139,101 (M<sup>+</sup> - (CoCp\*<sub>2</sub>)). CV (MeCN) V: *E*<sub>1</sub> = -0.93 (reversible), *E*<sub>2</sub> = -0.47 (irreversible oxidation).

**Supporting Information Available:** The molecular structures of **3–6** obtained from single crystal X-ray structure determinations, the geometry optimised structures of **1** and **7** and calculated isosurfaces of selected molecular orbitals of **1** and **7**. This material is available free of charge via the Internet at <http://pubs.acs.org>.